Wrapped Microstrip Antennas for Laptop Computers

J. Guterman[1,2], A. A. Moreira[1], C. Peixeiro[1], and Y. Rahmat-Samii[2]

[1] Instituto de Telecomunicações, Instituto Superior Técnico, TULisbon
Av. Rovisco Pais 1, 1049-001 Lisbon, Portugal
Tel: +351218418477; Fax: +351218418472; E-mail: {jerzy.guterman, antonio.moreira, custodio.peixeiro}@lx.it.pt

[2] University of California
Los Angeles, CA 90095-1594 USA
Tel: +1 (310) 206-2275; Fax: +1 (310) 206-4833; E-mail: rahmat@ee.ucla.edu

Abstract

The objective of this article is to provide a comprehensive and unified description of the authors' work on the development of wrapped microstrip antennas for laptop applications. The first contribution is the introduction of quasi-omnidirectional wrapped-microstrip antenna elements to be integrated into the display rim of laptops. Single- and dual-band antennas are presented to demonstrate the capabilities of wrapped microstrip antenna elements in wireless communications. The prototyping and measurements of these antennas are highlighted in an appendix. The most common internal and external laptop antenna structures are also described, to give a broader overview of laptop antenna-design approaches. The second and third contributions are a methodical analysis of housing effects, and a general study of electromagnetic human interaction with laptop antennas from the antenna-performance-degradation and user-illumination perspectives. These studies have been performed systematically for several classes of internal and external antennas, with different locations and screen-opening angles. With this approach, a general overview of laptop-antenna integration aspects is given, along with unified guidelines for the design of the wireless interface used in modern laptops. An application of the novel elements to capacity-preserving MIMO arrays is also presented.

Keywords: Laptop antennas; mobile antennas; microstrip antennas; compact antennas; multi-band antennas; wireless LAN; housing effects; electromagnetic human interaction; radiation effects; SAR; MIMO systems

1. Introduction

In the information-society age, computers play a fundamental role in the creation, distribution, and use of information. Due to very important advantages such as mobility, portability, and ever-decreasing prices, laptop computers are clearly taking the lead. Some of these advantages can only be fully realized together with wireless interfaces. A report on consumers' behavior from July 2006 [1] indicated that 39% of the surveyed population considered the added convenience of wireless computing one of the main reasons to buy a laptop.

Although the common need of working online everywhere and all the time may be questioned [2], and the majority of laptop wireless users work in a limited number of locations, the use of wireless gives the laptop operator a high degree of freedom and comfort, and is being applied to a growing number of solutions. Radio interfaces are widely used to connect with peripheral devices [3] (wireless personal-area networks, WPANs) and other computers [4] (wireless local-area networks, WLANs). The integration of cellular network radios into some modern laptops gives the user access to the Internet in areas not covered by WLANs. Ultimately, in a not-distant future, introduction of digital video broadcasting (DVB) television receivers and 60 GHz ultra-wideband transceivers [5], built into portable computers, is expected. The fast development and expansion of laptop wireless systems is driving the evolution of integrated antennas. Moreover, the required laptop miniaturization and aesthetics impose additional design constraints. A variety of new antennas developed for laptop computers has therefore been investigated. These designs have to meet specific requirements, while facing device-housing integration effects and operation in the proximity of the user.

In this article, we present an overview of the important steps of a successful laptop-antenna subsystem development. A new radiator-design methodology in laptop microstrip antennas, recently developed at the Instituto de Telecomunicações/Instituto Superior Técnico, Portugal, in cooperation with ARAM Laboratory, UCLA, will be described in Section 2. In addition, to give the reader a broader overview of laptop-antenna design approaches, the most popular commercially viable internal and external laptop antenna structures are introduced in Appendix 1. Laptop-housing effects and antenna-integration issues are studied in a wide range of scenarios in Section 3. Finally, Section 4 addresses electromagnetic human interaction with laptop antennas, analyzed from the antenna-performance and human-EM-exposure viewpoints. In addition, laptop-antenna fabrication and measurements are dis-

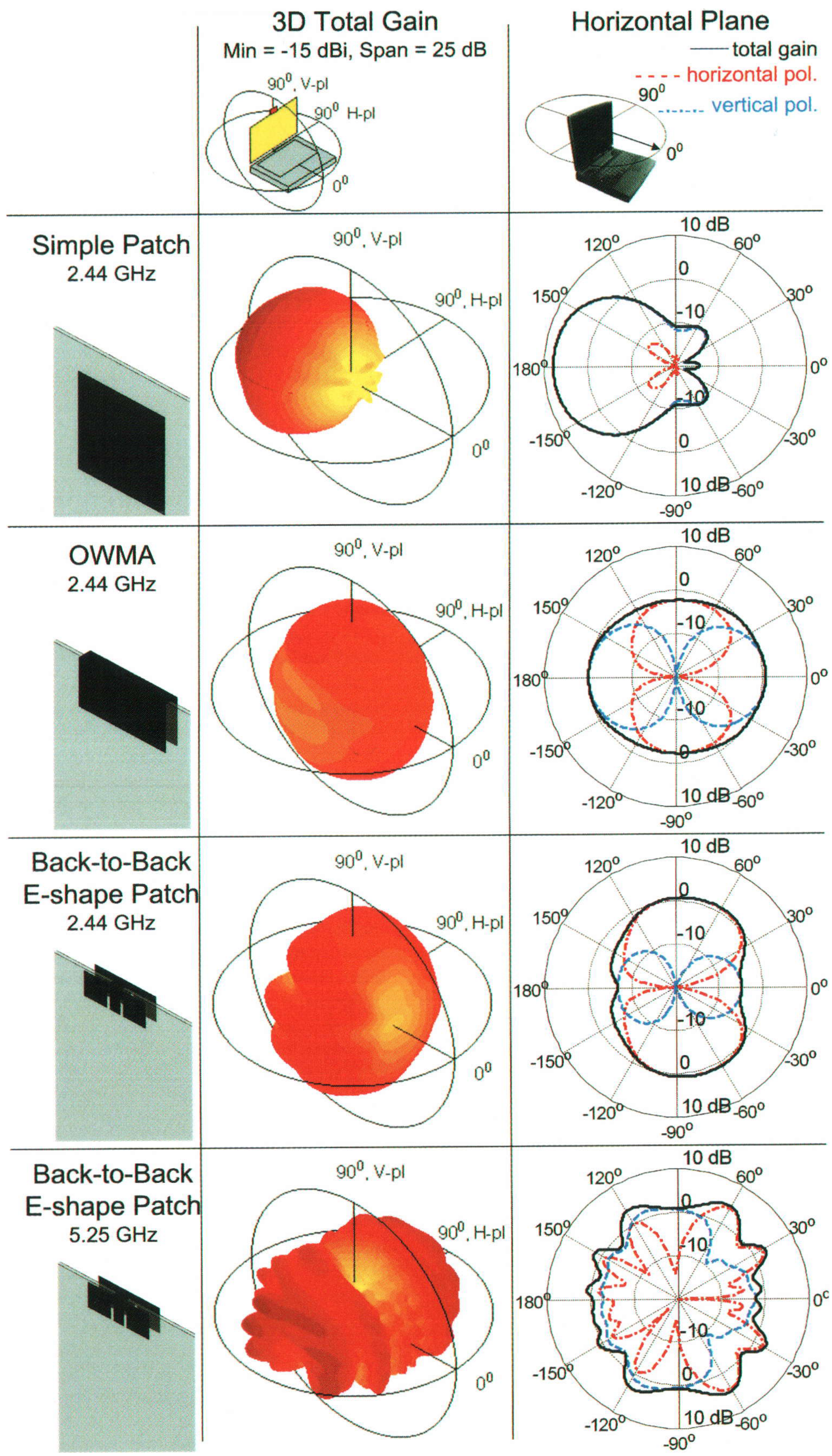

Figure 2. The calculated far-field gain patterns of microstrip antenna elements for laptops (the patches were integrated into a 14 in ground plane, without keyboard).

cussed in Appendix 2. Multiple-element antenna arrangements for MIMO-enabled laptops are outlined in Appendix 3.

1.1 Laptop Antenna Requirements

The antenna constitutes an interface between the electrical signals processed by the wireless subsystem front end and the wireless channel. To assure optimal transmission conditions, a laptop antenna should meet the following requirements:

- Sufficient impedance match: For laptop antennas operating in the transmitting mode, this guarantees that the reflection of RF power from the antenna port stays at an acceptably low level, which affects the system efficiency and therefore the battery lifetime. In the receiving mode, a good antenna impedance match improves the receiver's sensitivity.

- Multi-band operation: Due to the high integration scale, a single antenna element is often used to operate in more than one wireless system. It must provide a sufficient impedance match over several frequency bands. Some typical examples include dual-band 2.4 GHz/5.2 GHz [6, 7] and triple-band 2.4 GHz/ 5.2 GHz/5.7 GHz WLAN antennas [8, 9].

- Omnidirectional radiation pattern: This is the most adequate type of radiation pattern for laptop applications. It provides reliable wireless connectivity, independently of the terminal's orientation. As laptop computers are usually used in the horizontal position, the horizontal-plane radiation pattern is the most important.

- Antenna polarization: This is usually not a critical parameter for laptop applications, since laptops are used primarily in indoor environments, where there are intensive reflections and scattering [10].

1.2 Design Constraints and Challenges

Antennas for laptops, both in the case of external and internal solutions (see Appendix 1), are closely incorporated within the PC's structure, and their integration into the laptop plays a key role. There are three major challenges for antenna design associated with wireless integration into laptops:

- Miniaturization: Although it seems that miniaturization is of much less importance than in the case of handsets, laptop antennas have to be integrated within very densely packed electronic devices, where there is little room for additional functions. The size, shape, and location of the antenna may be affected by other design constraints, such as mechanical and industrial design [10]. The integration may be particularly challenging in the new, very small, ultra-portable laptops, and when multiple antenna arrangements are considered.

- Aesthetics: This is an important factor for consumers. Antennas should not brake the laptop's sleek design lines. In general, mechanically less-robust retractable antennas are substituted for by internal antennas, invisible to the user [10].

- Low profile: To minimize radiation from very high speed electronics, today's laptop computers are equipped with conducting covers or metallic shields, just inside the plastic covers [10]. This condition, imposed by FCC Part 15 Subpart B emission requirements, significantly affects the antenna design, as it is difficult to place an antenna in an environment free enough of other conductors to create an efficient radiator. It is also a motivation to use microstrip-type antennas in laptops, as will be detailed in Section 2.

The design of a laptop integrated antenna that meets all the requirements and constraints described above is a challenging task. The antenna's final performance depends not only on the structure of the radiating element, but also on the antenna's location within the laptop, and on other nearby components. Finally, the presence of the user also affects the antenna's operation, and needs to be taken into account.

2. Microstrip Antennas for Laptops

The laptop structure plays a key role in the antenna system's operation. First, it restricts the radiator's shape and size. Second, due to the inherently distributed character of the antenna, it participates in the radiation mechanism. An understanding of the behavior of the laptop's constituent parts in the microwave regime will allow not only accurately forecasting the effects of the laptop's housing (for a given antenna, as discussed in Section 3), but will also allow designing the antenna element that can achieve the best performance the laptop integration can offer.

Many antenna systems used in laptops can be considered to be "dipole-like." The antenna itself is one part (a monopole), and the other part (the image) is provided by the laptop [10]. Therefore, the laptop's structure can be treated as an expansion of the antenna's ground plane, as in the case of slot antennas [11]. Furthermore, some antenna designers consider the laptop to be the basic antenna, and the antenna element itself to be a tuning element. However, this approach is more common in handset terminal design, where the dimensions of the antenna element and housing are very much comparable [12]. Typical laptop terminals have a clamshell form, comprised of a keyboard (chassis) and a display (lid), with maximum dimensions in the range of several free-space wavelengths (for WPAN/WLAN frequencies of operation). Due to the relatively large electrical size and the above-mentioned extensive use of conducting shields, both keyboard and screen can be approximated by metal boxes, as shown in [13-15]. Taking into account that the metallic surrounding limits the thickness of the available space for a radiator, microstrip antennas seem to be ideal candidates for a laptop's built-in wireless interface. Microstrip antennas need a ground plane, and due to their conformal properties and low profile, they can be easily integrated between the metal shielding layers and the plastic cover.

The backside of a laptop's display has plenty of space for microstrip-antenna integration. However, a simple patch antenna (Figure 1a), when printed over the relatively large ground plane, basically radiates towards the back hemisphere of the display (a front-to-back ratio above 15 dB) [16], even when the patch approaches the display's edge [17]. The radiation pattern of such a patch antenna (Figure 2, top row), is far from omnidirectional which is not adequate for the envisaged application (see Section 1.1). In order to balance forward and backward radiation, the

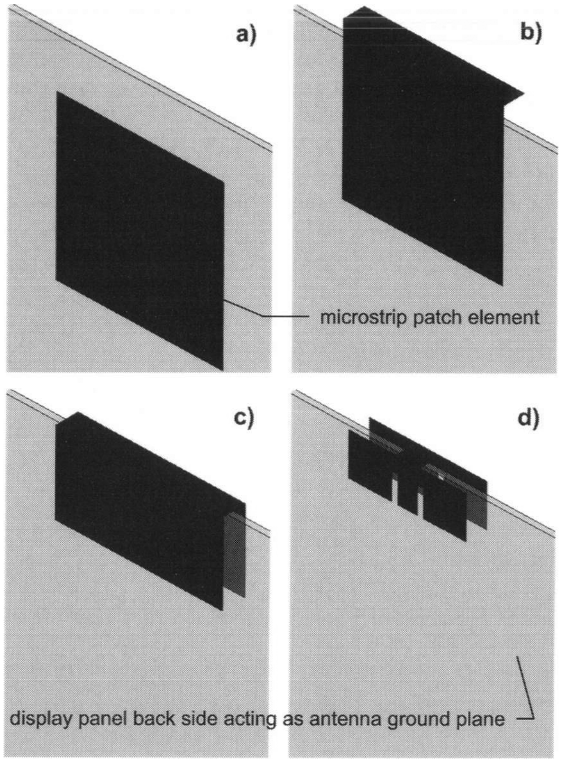

Figure 1. The evolution of microstrip patch antennas for laptops: a) a simple half-wavelength patch mounted on the laptop display's back side [16, 17]; b) an L-bent protruded patch antenna [18]; c) an omnidirectional wrapped patch antenna [19]; d) a dual-band back-to-back E-shaped antenna [21].

patch antenna can protrude above the ground plane's edge (Figure 1b). Moreover, by adding a bent section, its bandwidth can be expanded [18]. This solution, denoted as an L-Bend protruded patch, can reduce the front-to-back ratio to 2.7 dB.

2.1 Omnidirectional Wrapped-Microstrip Antenna (OWMA)

An omnidirectional wrapped-microstrip antenna (OWMA) has been proposed to improve the front-to-back ratio to values as low as 0.5 dB [19]. The antenna's schematic structure and ISM 2.4 GHz prototype are shown in Figure 1c and Figure 3, respectively. The patch element consists of three segments: identical front and back sections, and a connecting top section. Very good antenna omnidirectional performance is obtained due to the front-back symmetry. The wrapped patch element conformably embraces the ground plane, leading to a more compact configuration.

The omnidirectional wrapped-microstrip antenna operating mechanism can be explained with the aid of the patch's surface-current distribution, shown in Figure 4b. The comparison with the current distribution in a simple microstrip patch (Figure 4a) clearly shows the resemblance of the excited modes. Therefore, the total "unwrapped" electrical length of the omnidirectional wrapped-microstrip antenna is approximately 0.5λ. The two equivalent radiating slots [20] are located on the opposite sides of the ground plane, leading to a small front-to-back ratio. Moreover, the front and back wrapped-patch sections are shorter than a quarter wavelength, providing an easier integration within the laptop's screen (see the ISM 2.4 GHz prototype compared with modern laptop screen housing in Figure 3). The fabrication technique, feeding methods, and measurement procedure for the antenna are described in Appendix 2.

The omnidirectional wrapped-microstrip antenna concept can be applied directly to a simple rectangular patch, leading to a sin-

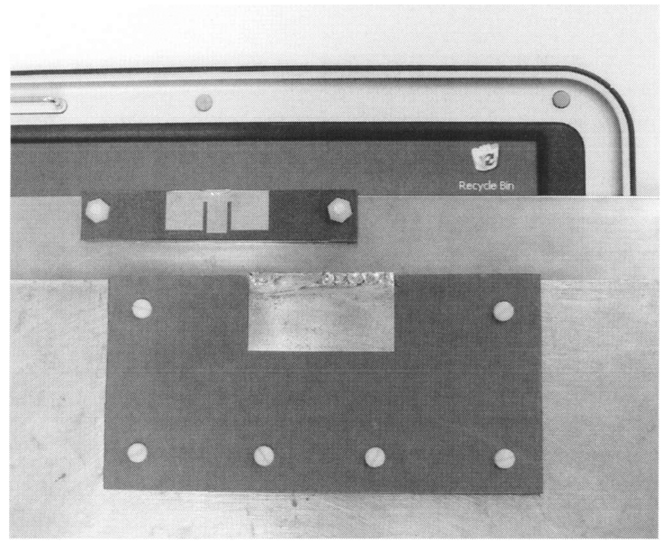

Figure 3. Single- and dual-band microstrip antenna prototypes compared with a modern laptop screen casing (HP Compaq nx9110).

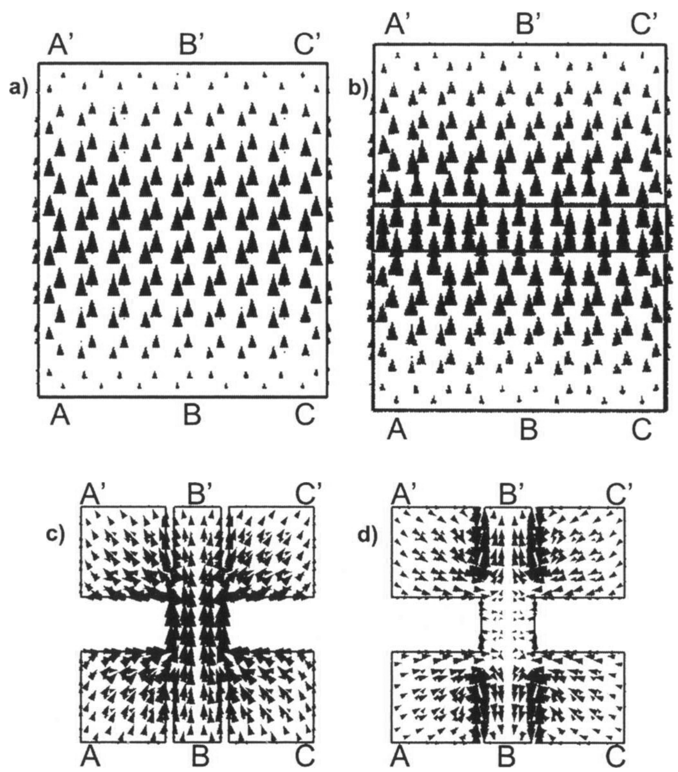

Figure 4. The current distributions in microstrip elements, with the patches shown as "unwrapped:" a) a simple patch in the first mode, b) an omnidirectional wrapped-microstrip antenna (OWMA) in the first mode, c) a back-to-back E-shaped patch in the first mode, d) a back-to-back E-shaped patch in the second mode.

gle-band design, as presented in [19]. The 2.4 GHz antenna prototype has been fabricated and integrated into a W×H×T = [295 × 225 × 1] mm^3 metal plate, which mimics a 14 in TFT panel. Despite of the electrically large ground plane, the antenna radiates almost omnidirectionally (Figure 2, second row). For the configuration described in [19], the operating bandwidth (where $S11 < 6$ dB) was 5%, which is sufficient to cover the popular ISM 2.4 GHz band. The 2.4 GHz omnidirectional wrapped-microstrip antenna design will be used for the antenna-housing (Section 3) and the human-interaction studies (Section 4).

The front-to-back symmetry can be also applied to more-convoluted patch shapes, giving additional freedom in antenna miniaturization and multi-band design, while keeping a quasi-omnidirectional horizontal-plane pattern, as described in the next section.

2.2 Dual-Band Back-to-Back E-shaped Patch Antenna

A dual-band back-to-back E-shaped patch antenna was proposed in [21]. It combines the concepts of the omnidirectional wrapped-microstrip antenna and E-shaped patch elements [22], leading to the geometry shown in Figure 1d. As for the omnidirectional wrapped-microstrip antenna, the patch element consists of three sections: two identical front and back sections, and a top connecting section. In the case of the dual-band antenna, the front and back elements are "E" shaped, which allows for dual-band operation and miniaturization. The top connecting section is narrowed, in order to assure additional tuning and further antenna miniaturization [21].

As in the case of the omnidirectional wrapped-microstrip antenna, the operation mechanism of the proposed antenna can be explained with the aid of the surface-current distribution on the patch, shown in Figure 4. In the lower resonant mode (Figure 4c), the main current paths expand between points $B\text{-}B'$, $A\text{-}A'$, and $C\text{-}C'$; the slots practically do not affect the antenna's operation, as they are parallel to the current lines. This mode is analogous to the higher resonant mode of the simple E-shaped patch antenna [22], but in the back-to-back configuration, the two resonant lengths of the simple E-shaped antenna are connected in series by the connecting strip. In the higher resonant mode (analogous to the lower resonant mode of a simple E-shaped antenna [22]), Figure 4d, the main current lines expand around the slots: between points $A\text{-}B$, $C\text{-}B$, $A'\text{-}B'$, and $C'\text{-}B'$.

The ease of antenna tuning deserves particular attention. It has been demonstrated [21] that for a fixed external dimensions of the antenna patch (often limited by other design constraints), two resonant frequencies can be tuned almost independently in a fairly broad range, $f_2/f_1 \in [1.2, 3.5]$, by modification of only the slot lengths and the connecting-strip width. This feature may be also used in the future to fabricate reconfigurable antennas with MEMS switches [23].

The design and testing of a 2.4/5.2 GHz antenna was described in detail in [24]. The antenna's input matched bands ($S11 < -6$ dB) covered, with margins, the ISM 2.4 GHz and the UNII 5.2 GHz bands (Figure 5), popularly used in WLANs. Despite the relatively large ground plane, the antenna has fairly omnidirectional horizontal-plane total gain patterns in both operating bands (Figure 2). In the 2.4 GHz band, the three-dimensional pattern is similar to that of the 2.4 GHz omnidirectional wrapped-microstrip antenna. The decreased radiation in the broadside forward and broadside backward directions (0° and 180° in the horizontal pattern) is caused by the cancellation of horizontal E-field components (notice the left-right symmetry of current distribution in the E-shaped sections, Figure 4c). The far-field radiation pattern in the 5.2 GHz band reminds one of the pattern of a vertical dipole, which is optimum for wireless communications (the maximum radiation lays at angles close to the horizontal plane, corresponding to maximum distances between the mobile unit and the access point). The 2.4/5.2 GHz back-to-back E-shaped antenna design will be used in the antenna-housing (Section 3) and the human-interaction studies (Section 4).

3. Antenna Integration Aspects

In Section 2, microstrip antenna elements for laptops were described. In addition, some typical commercial laptop-antenna solutions are addressed in Appendix 1. Their characteristics – namely, their radiation pattern and radiation efficiency – however, depend on the radiator's location in the laptop [10, 25], and on the antenna's position with respect to the surrounding dielectric and metal structures [10, 26]. The overall built-in system performance is also affected by the distance between the RF front end and the antenna: a 0.5 m section of miniaturized coaxial cable operating at 5 GHz may introduce a 3 dB loss. The antenna's location therefore plays a critical role in the laptop's wireless interface performance, and has to be designed with special care. Moreover, for some antennas, the input matching may depend on the antenna's location: the element may therefore have to be tuned after integration into the laptop. In this section, the characteristics of typical antenna locations for plug-in and built-in interfaces are discussed. The most common locations are depicted in Figure 6.

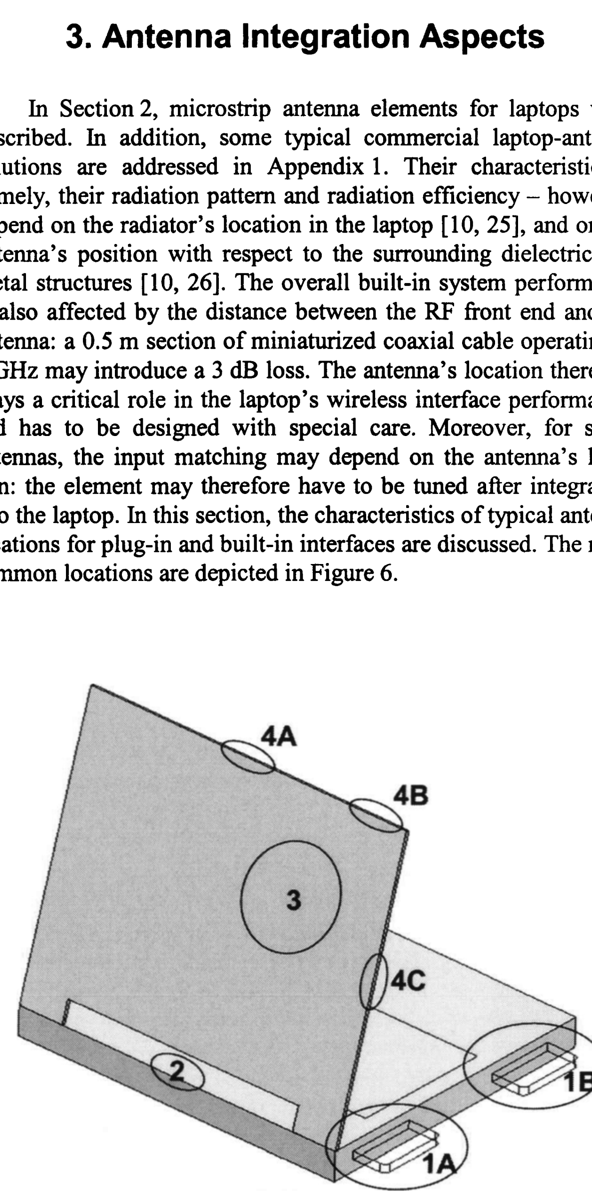

Figure 6. Common locations and corresponding applicable antenna types in a laptop. External antennas: 1A, 1B: plug-in interface: sleeve dipole, monopole, inverted-F antenna (IFA), planar inverted-F antenna (PIFA), chip antenna. Internal antennas: 2: base-mounted antenna: PIFA, chip antenna; 3: screen back side: microstrip patch antenna; 4A-C: screen rim: IFA, flat-plate antenna, miniaturized monopoles, wrapped patch antenna, chip antenna.

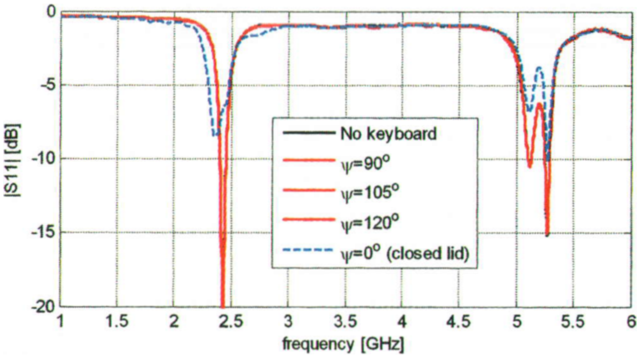

Figure 5. Keyboard effects on the measured input reflection coefficient of a middle-top mounted back-to-back E-shaped patch antenna.

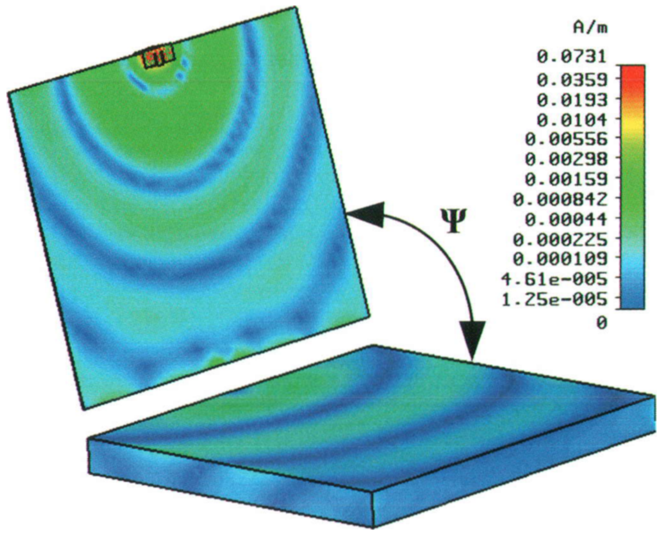

Figure 7. The surface-current distribution in the laptop's metallic elements at 2.44 GHz.

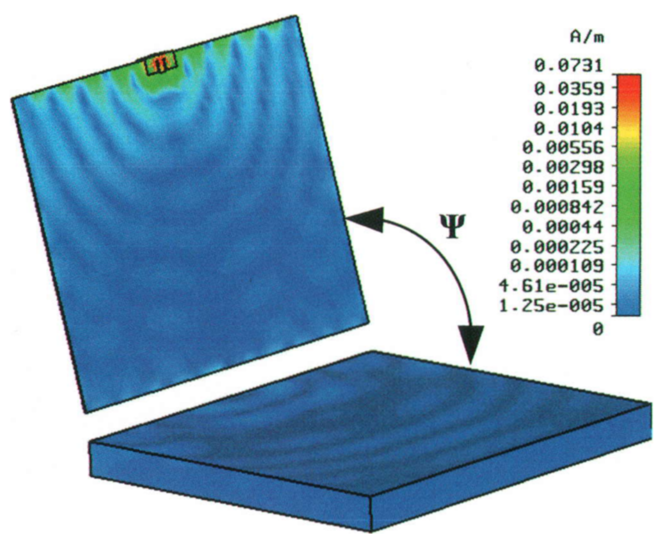

Figure 8. The surface-current distribution in the laptop's metallic elements at 5.25 GHz.

3.1 Laptop Housing Effects: Internal Antennas

The integration of internal laptop antennas gives the designer a much wider choice of element locations than in the case of antennas for plug-in interfaces. The designer may also have access to details of the entire laptop structure. Housing effects can therefore be better predicted and taken into account. Early studies evaluated possible antenna locations, independently of the antenna's element type, with the aid of the electromagnetic visibility study (EVS) technique [25]. This method is based on illuminating the laptop structure with a plane wave, incident from a variable angle, and monitoring the excited surface-current density at the points of interest. The best antenna locations are those where the surface-current density is the highest, and are less dependent on the illuminating-wave's incident angle. The best results were obtained for location 4A (see Figure 6). Next in the ranking were locations 4B, 4C, and 3 [25, 27]. Locations 1A, 1B (housing of external antennas will be discussed in Section 3.2), and 2 were classified low in the electromagnetic visibility study ranking.

The electromagnetic visibility study results showed that the locations on top of the display lead to an antenna performance that is almost similar to free space [27]. For those positions, the influence of the laptop's structure on integrated antenna's operation is minimized, but not eliminated. The mechanisms affecting the performance of built-in antennas are discussed below, for the 2.4/5.2 GHz back-to-back E-shaped antenna.

The analysis presented in Section 2 assumed an integration of the laptop antenna in the middle top edge (location 4A in Figure 6) of a 14 in metal plate, which mimicked the TFT panel. In practical applications, the laptop's screen is mounted over a keyboard base, which breaks the front-to-back symmetry. Due to other design constraints, the laptop antenna may have to be integrated in other locations. The influence of the laptop's structure on the back-to-back E-shaped antenna's performance will be discussed below for representative screen antenna locations (4A, 4B, and 4C in Figure 6), and for different laptop-screen opening angles. The results of the numerical simulations will be compared with measured data (using a real laptop model). Details of antenna prototyping and measurement can be found in Appendix 2.

In the microwave frequency range, the laptop's keyboard base behaves as a metallic box [13, 14], and can be treated as an expansion of the laptop antenna's ground plane. It significantly affects the antenna's performance, due to shielding and reflection of the electromagnetic waves radiated by the antenna. The simulated current distributions in the laptop body's metallic elements are presented in Figure 7 (at 2.44 GHz) and Figure 8 (at 5.25 GHz). It can be observed that significant surface currents are induced in the entire screen and keyboard base, and the whole laptop body therefore acts as an antenna.

The measured antenna-input reflection coefficient for the middle top (4A) antenna location and for different screen-opening angles is presented in Figure 5. As can be seen, the antenna's matching properties were practically independent of the screen-inclination angle (all solid curves overlapped), unless the lid was completely closed (the dashed curve). A similar study was performed numerically and experimentally for the omnidirectional wrapped-microstrip antenna [13], back-to-back E-shaped and inverted-F (IFA) antennas, for all screen locations 4A-4C, and the same conclusion was obtained. This feature is very useful for the antenna designer: in the antenna-matching procedure, the laptop base does not need to be modeled. This may drastically reduce the simulation complexity. Moreover, it has been found that the input matching of the omnidirectional wrapped-microstrip antenna and the back-to-back E-shaped antenna almost does not depend on the antenna's location, even when one radiator edge approaches the screen's corner [29].

The three-dimensional simulated and measured total gain far-field radiation patterns are shown in Figure 9 (at 2.44 GHz) and in Figure 10 (at 5.25 GHz). In addition, principal-plane cuts are presented, to facilitate the quantitative interpretation of the results. Very good agreement was obtained between numerical simulations and measured results, which validated the simple PEC box model of a laptop (see Appendix 2).

The first rows of Figure 9 and Figure 10 show the far-field radiation patterns of the antenna attached to the laptop's screen (represented here as a metal plate), without the keyboard base (Figure 11a). According to Section 2.2, in the lower frequency band (Figure 9), the antenna radiates almost omnidirectionally, while in the higher band it has a dipole-like pattern (Figure 10). The introduction of the keyboard significantly affects the radiation pattern. This effect is more pronounced in the front screen hemisphere, where the wave radiated directly from the antenna interferes with the wave reflected in the keyboard. The elevation locations of maxima and minima depend on the laptop's opening angle (compare rows 2 and 3 in the figures). The antenna's location influences the horizontal pattern (see rows 2 and 4). The keyboard effect in the back screen hemisphere is small. In the higher frequency band, the keyboard effect is less pronounced, because the back-to-back E-shaped antenna radiation towards the keyboard is relatively low (compare the patterns for 2.4 GHz and 5.2 GHz in row 1).

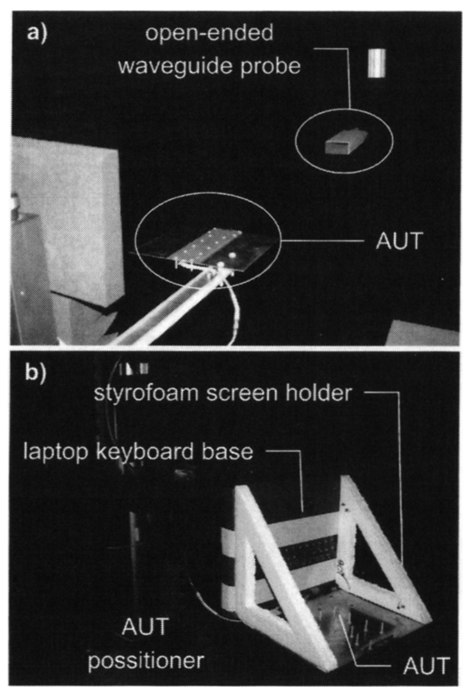

Figure 11. The antenna-measurement setup in the UCLA spherical near-field facility: a) the standalone antenna, b) the antenna attached to a real laptop keyboard base.

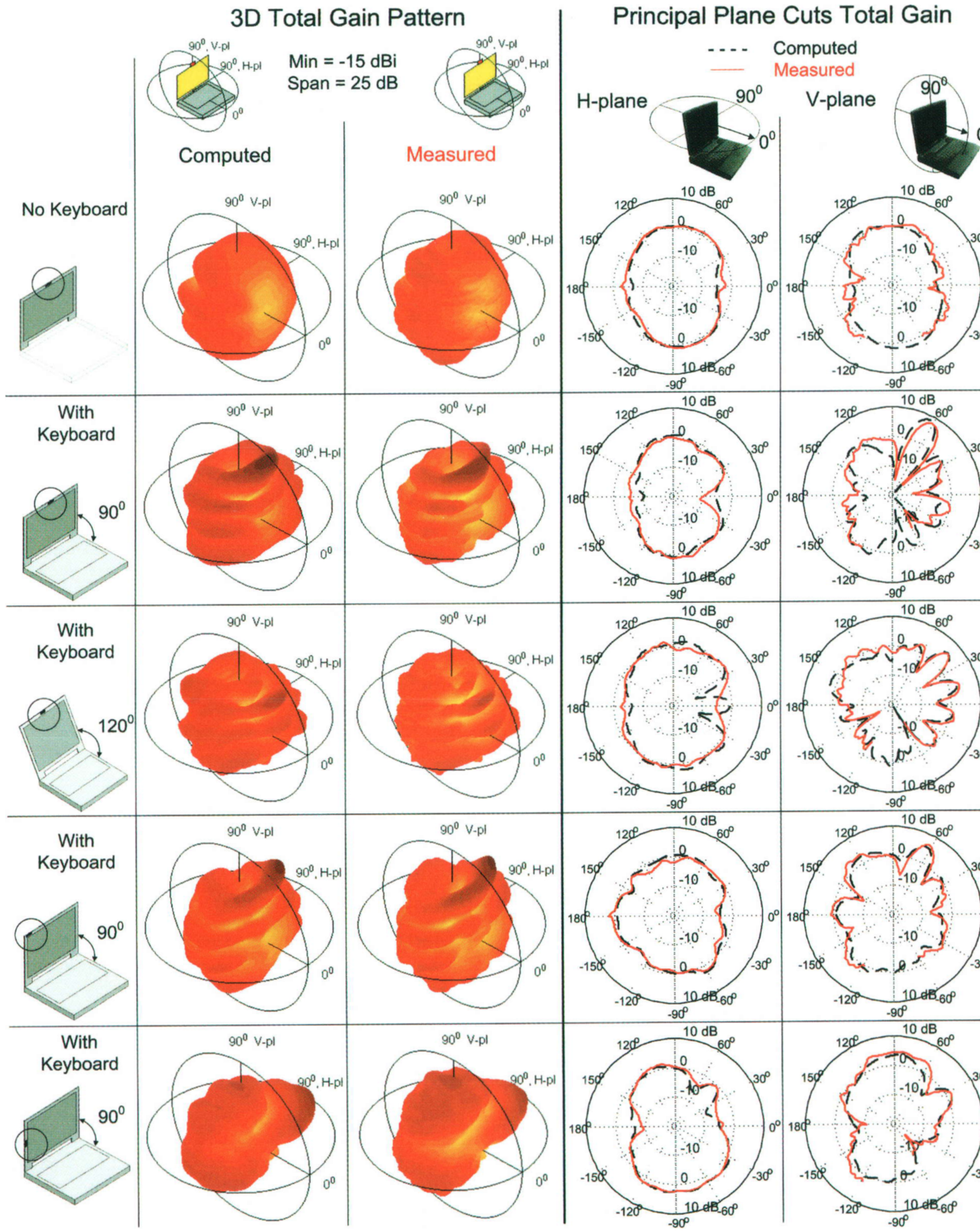

Figure 9. The far-field gain patterns of an E-shaped back-to-back antenna integrated into a laptop for different antenna locations and screen-opening angles at 2.44 GHz (the first row shows the antenna's performance without the keyboard, for comparison).

For all the considered top-edge screen locations, the antenna showed a quasi-omnidirectional horizontal-plane total gain pattern, which is generally required for mobile communication applications. When the antenna was mounted over a side screen edge, the omnidirectional behavior was lost, especially in the higher frequency band. The same radiation-pattern study has been performed for screen-integrated omnidirectional wrapped-microstrip antenna [13] and inverted-F antenna elements, and similar conclusions have been derived.

The analysis assumed integration of the microstrip antenna with a metal plate that mimicked the TFT panel. In a more-realistic scenario, the radiator vicinity has a more complex form, and also affects the antenna's operation. The plastic cover layers modify the effective permittivity of the antenna's neighborhood, and therefore affect the antenna's physical size. Moreover, the dielectric losses in the plastic cover decrease the radiation efficiency. When the laptop case consists of a very lossy material (for instance, carbon-fiber-reinforced plastic, CRFP) it may even be necessary to design a special "RF window" for the antenna [11].

3.2 Laptop Housing Effects: External Antennas

External antennas are usually integrated in plug-in platforms, which expand the functionality of laptops. Initial implementations – still very popular – used PCMCIA-card expansion slots, whereas recent radio interfaces are integrated inside miniature USB dongles. In these platforms, the antenna-location choice is very limited, and it does not allow laptop-independent performance. The antenna is usually integrated in the most-distant location of the card section, protruding from the laptop, in order to reduce the effect of the laptop itself on the communication link's performance.

Typical plug-in interface locations include 1A and 1B (Figure 6), for both PCMCIA and USB dongle housings. For those representative locations, numerical analyses of a PCMCIA-housed ISM 2.4 GHz sleeve-dipole antenna and inverted-F antenna element (see Appendix 1) were performed. As a reference, the performance of a freestanding-antenna-plus-PCMCIA setup was evaluated [30]. In those examples, the laptop's opening angle was $\psi = 90°$. It was noted that the antenna's input matching was affected by the laptop's body (see Figure 12), because the body disturbed the electromagnetic fields in the very close vicinity of the radiator. As the plug-in interface manufacturer has no detailed information about the card's location, the manufacturer must assure sufficient bandwidth margins to overcome potential detuning.

As shown in Figure 13, and in agreement with the electromagnetic visibility study technique results (Section 3.1, [25]), the antenna's radiation pattern is strongly dependent on the antenna's location. The sleeve-dipole antenna possesses an omnidirectional radiation pattern when mounted vertically on a relatively small PCMCIA card (Figure 13, first row). When attached to the laptop, the far-field radiation pattern is clearly modified, and differs significantly from omnidirectional. The laptop-screen shielding effect is visible for azimuth angles between 90° and 180°. The reflection from the screen contributes to an enhanced power radiation in the azimuth range of 0°-90°. As the distance between the antenna and the screen changes (the PCMCIA card is moved from location 1A to 1B), the interference pattern visible in this angular range also changes. This phenomenon can be intuitively explained with the aid of a virtual antenna array, constituted by the sleeve dipole and its image, representing the reflection from the screen. When the antenna's spacing increases (from below a half-wavelength in 1A to over two wavelengths in 1B), several lobes appear in the radiation pattern. The vertical radiation pattern, although of less importance for laptop applications, is also affected by the presence of the laptop's structure.

The horizontal-plane radiation pattern of an inverted-F antenna element, integrated into a freestanding PCMCIA card, is less omnidirectional than the pattern obtained for the sleeve dipole (compare the first and fourth rows of Figure 13). However, the inverted-F antenna element is more robust to the influence of the laptop's structure. As the antenna is mounted in the keyboard's base plane (below the screen), the display-panel shielding and reflection effects are not so pronounced as for the sleeve dipole. Other antenna types, integrated into the card's circuit board, such as chip antennas, possess the same advantage. However, the effects of the laptop's structure on the antenna's performance also depend on the antenna's dominant polarization, and have to be evaluated separately for each antenna type.

In the simulations, simplified laptop and PCMCIA card models composed of PEC boxes were assumed. In practical applications, the antenna's performance is particularly affected by the lossy plastic case, and depends on the antenna's separation from the laptop's body. An experimental study has shown that by extending the default PCMCIA card protrusion by 6 mm, the antenna's sensitivity may be improved by almost 6 dB, which corresponds to an over 60% range expansion [10]. The radiation efficiency of an antenna integrated inside the plug-in card also strongly depends on the dielectric losses inside the printed-circuit board and the device's plastic case.

The common disadvantage of on-card-mounted (locations 1A, 1B) and keyboard-base-mounted (location 2) antennas is the influence of the external environment, such as a metal desk and/or the user, on the antenna's performance [27]. A metal desk may significantly shift the tuning of the antenna, and create unwanted reflections that change the radiation pattern. The absorption of electromagnetic energy by the user's hands and lap can have a dramatic effect on the antenna's gain, as described in Section 4.4 and in [10]. These effects are much less pronounced for antennas integrated inside the laptop screen (see Section 3.1), which pre-select those as the most-beneficial antenna locations [27].

4. User Interaction with Laptop Antennas

The electromagnetic (EM) interaction between humans and wireless-terminal antennas has been an important topic in the last fifteen years. Initially, the problem was studied for handsets, where the effects are very pronounced [30] due to the very small size terminal placed in the nearest vicinity of the operator. Nowadays, the human-terminal interaction has to be studied in a wide range of scenarios, due to three main factors: (i) the variety of portable units is expanding, (ii) the high wireless-link performance requirements force an accurate description of in-situ operation, and (iii) the public awareness of human exposure to electromagnetic radiation has grown.

As the distance between laptop antennas and the user is typically several wavelengths, this interaction seems intuitively of less importance than in handsets. However, it should be noted that

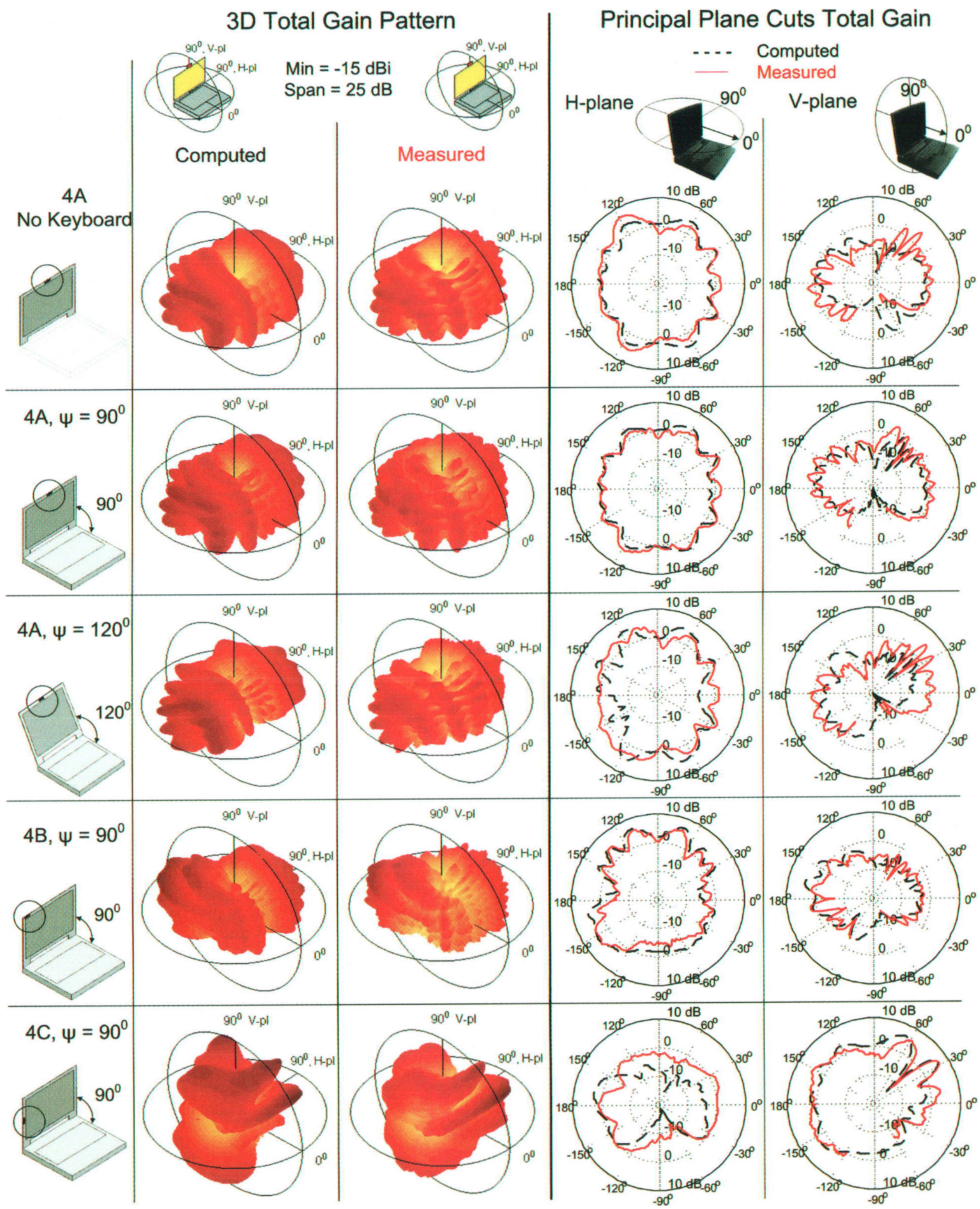

Figure 10. The far-field gain patterns of an E-shaped back-to-back antenna integrated into a laptop for different antenna locations and screen-opening angles at 5.25 GHz (the first row shows the antenna's performance without the keyboard, for comparison).

according to Section 3, the entire laptop's structure participates in the radiation mechanism, and the human belongs to the near-field zone of such a defined antenna-plus-laptop radiator. A typing user places his or her arms just above the metallic-keyboard layers, where significant currents are excited (see Figures 7 and 8). Moreover, the user's palms may closely approach antenna elements integrated in plug-in cards. As different antenna locations and screen-opening angles affect the radiation properties (Section 3), they will also affect the way the radiator interacts with the user.

In this section, the electromagnetic-human interaction with laptop antennas is analyzed in three steps, as shown in Figure 14. In Step 1 (Figure 14, column 1), the human interaction with a back-to-back E-shaped antenna (Section 2.2) is analyzed in detail for different element locations (4A, 4B, and 4C of Figure 6) [32] and for different screen-opening angles [33]. In Step 2 (Figure 14, column 2), results for different antenna element are compared [34]. In Step 3 (Figure 14, column 3), the interactions between the user and both an internal screen-mounted antenna and an external PCMCIA-card antenna (locations 1A and 1B) [35] are compared. In this step, an inverted-F antenna element is used, as it is commonly used in both external and internal designs. The comparisons between the antenna's freestanding and in-situ performance (measured in terms of input matching, far-field radiation pattern, and radiation efficiency) for each scenario, demonstrate the human's effect on the antenna's operation. The exposure of human biological tissues to electromagnetic radiation is analyzed in terms of Specific Absorption Rate (SAR).

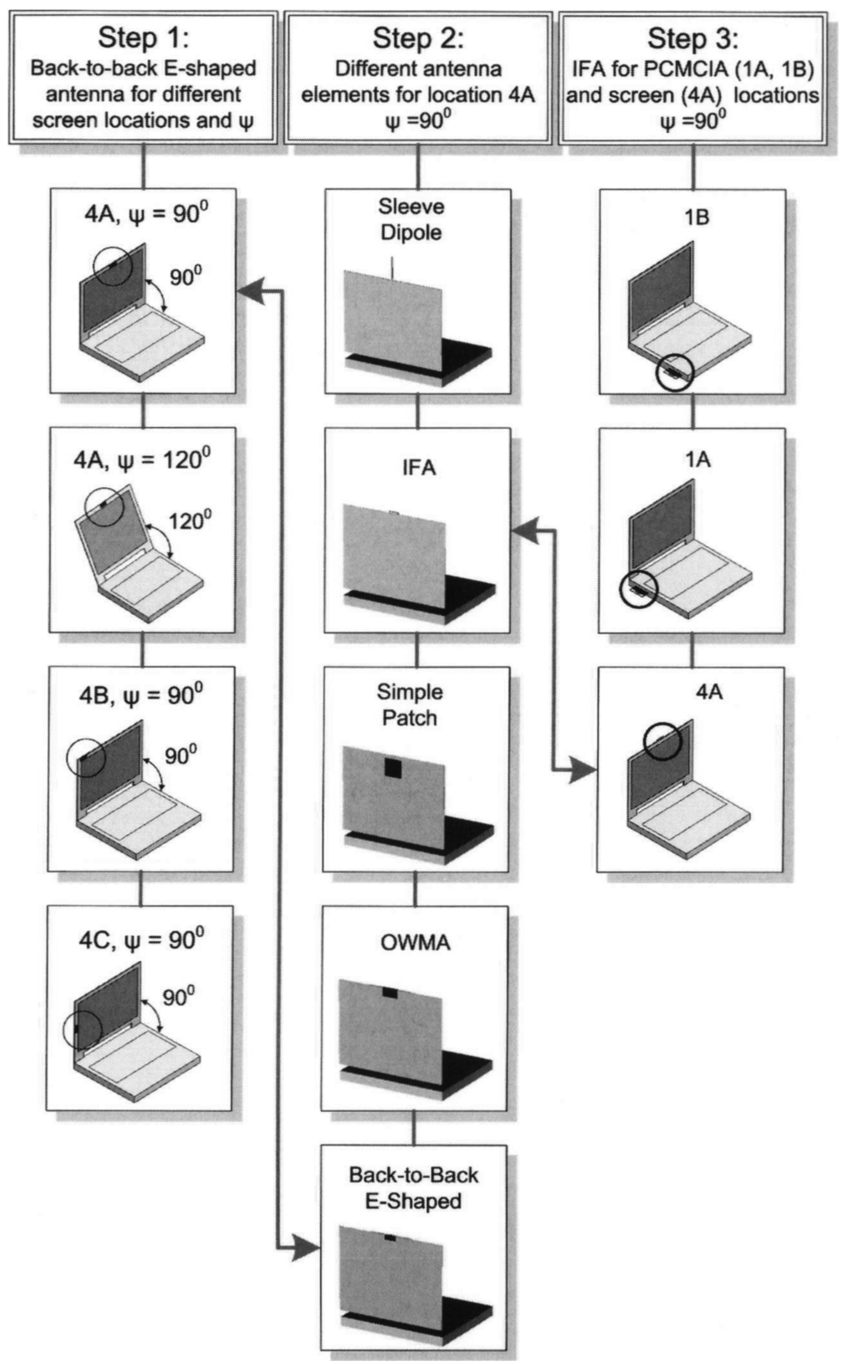

Figure 14. The organization of the EM human-interaction scenarios.

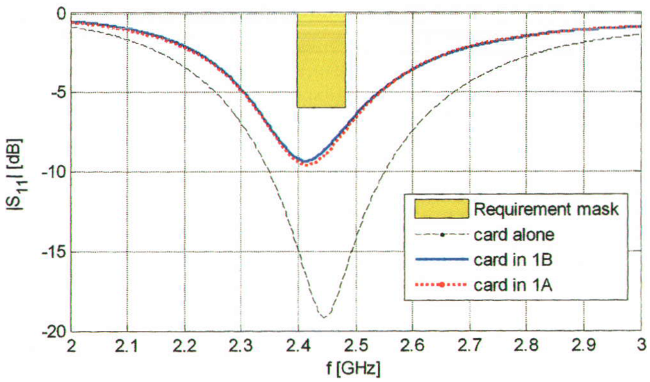

Figure 12. The effect of the laptop's housing on the input reflection coefficient of an inverted-F antenna (IFA) mounted in a PCMCIA card.

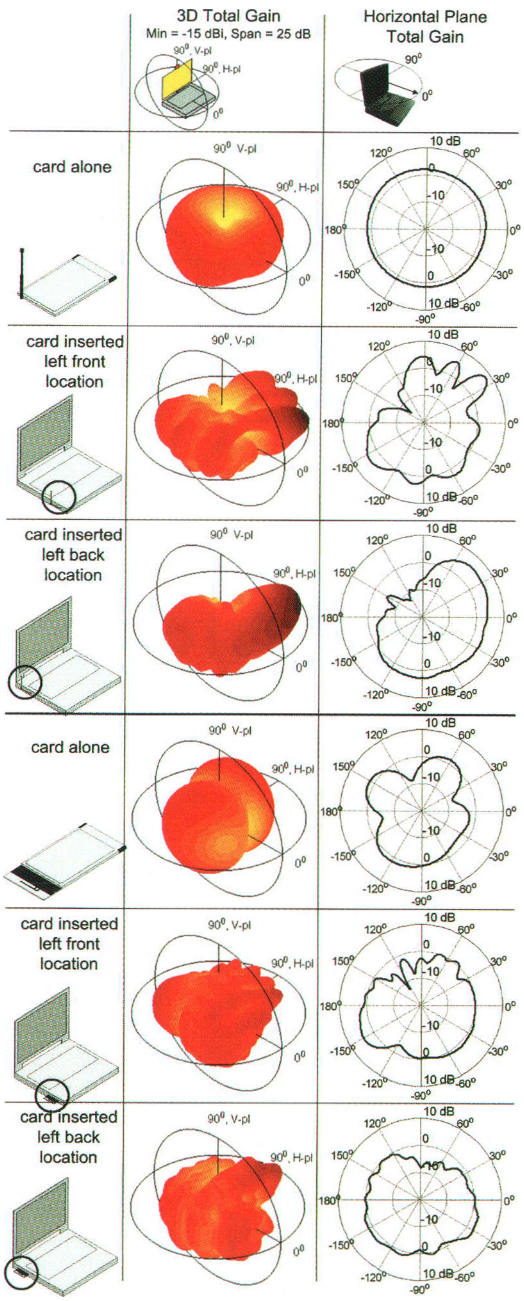

Figure 13. The 2.44 GHz computed far-field gain patterns of sleeve-dipole and inverted-F antenna (IFA) elements mounted on a PCMCIA card.

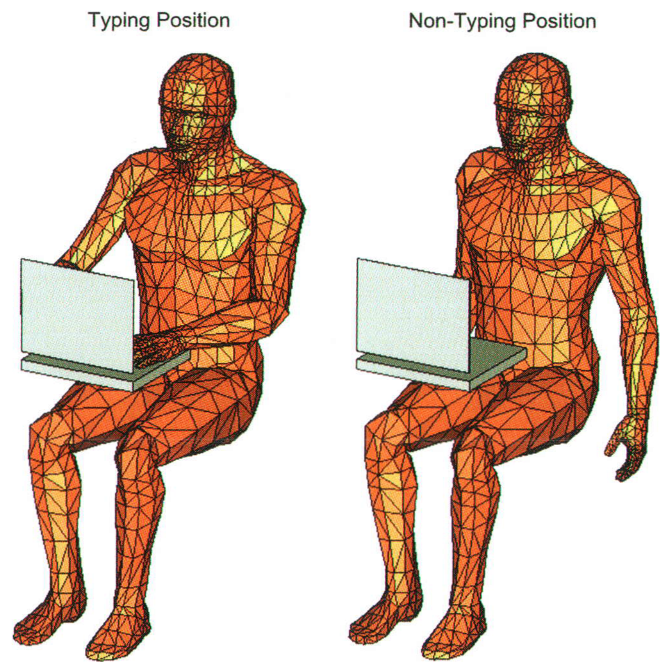

Figure 15. Two typical scenarios for the laptop-operator interaction.

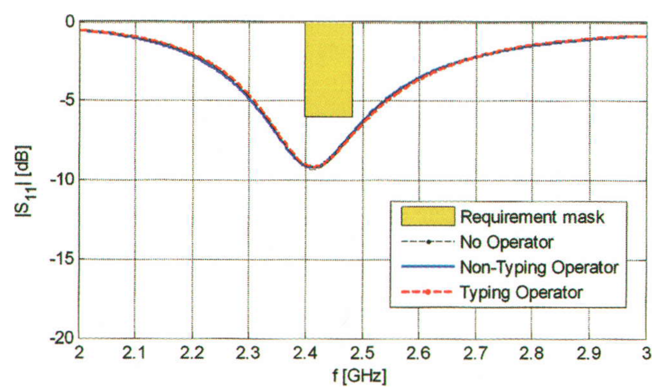

Figure 16. The effect of the laptop's user on the input reflection coefficient of an inverted-F antenna (IFA) mounted in the front keyboard location 1B.

4.1 Physical Modeling

The laptop-human interaction study was based on full-wave simulations performed with the CST *Microwave Studio* software tool, which implements a Finite Integration Technique (FIT) [36]. The antenna elements were integrated into the simplified laptop model, consisting of PEC display and keyboard setup, which has proven to be a good approximation to a real laptop housing (see Section 3). A human phantom, based on an anatomical mannequin corresponding to a male of height 177 cm and weight 72 kg, generated by the *Poser* software tool, was used in the numerical simulations. Typical typing and non-typing postures (Figure 15) were considered. Since only the external shape and size were used, the generated model was homogeneous. A dielectric material with a relative permittivity of $\varepsilon_r = 45.6$, a dielectric loss tangent of $\tan\delta = 0.23$, and a mass density of $\rho = 1000\,\mathrm{kg/m^3}$ was used to simulate the human biological tissue at 2.44 GHz. These values corresponded to averaged properties of 85% muscle and 15% fat, which may be representative of a healthy male [37]. Due to the large electrical size of the model, simulations were carried out only in the ISM 2.4 GHz band.

4.2 User Effects on Input Matching

The antenna's input impedance is a function of the field distribution in the nearest vicinity of the antenna's feeding point. It therefore is affected only when the currents excited in that area are disturbed, e.g., by the human's presence. The analysis of the antenna's input reflection coefficient has shown that for all the analyzed scenarios, the influence of the operator on the antenna's matching was negligible. In Step 1 (see Figure 14, column 1) it was observed that independently of the screen-integrated antenna's location [32] and of the lid-opening angle, Ψ [33], there was no effect of the laptop's operator on the antenna's input reflection coefficient. This observation was also confirmed for all the different antenna elements analyzed in Step 2 [34] (see Figure 14, column 2). Finally, in spite of the small distance between the PCMCIA inverted-F antenna in locations 1A and 1B and the typing user's arm (less than 4 cm, which is about a third of the free-space wavelength), the PCMCIA antenna's input matching was not affected by the human's presence [35], as presented in Figure 16.

4.3 User Effects on Radiation Pattern

Contrary to the antenna's input impedance (defined in the feeding point), the far-field pattern is an integral function of currents in the entire body of the laptop. As the laptop's user is located in the antenna's near-field zone, he/she will not only block and reflect the antenna's radiation (which could be accounted for in a Geometrical Optics approach), but will also disturb the current distribution in the antenna-and-laptop structure. The antenna, the laptop, and the user therefore need to be analyzed as a whole.

A comparison of far-field total gain patterns for all the scenarios of Step 1, Step 2, and Step 3 are presented in Figures 17, 18, and 19, respectively. As it has been noted that the posture (typing/non-typing) of the operator does not have an influence on the EM interaction with screen-integrated antennas (Step 1 and Step 2), Figures 17 and 18 present results only for the typing position.

The effects of the human operator on the 2.44 GHz far-field gain pattern of a back-to-back E-shaped antenna for different patch locations and different laptop-opening angles (Step 1) are shown in Figure 17. According to Figure 9, the radiation pattern of a freestanding laptop arrangement depends on the antenna's location and on the screen-opening angle. First, for $\Psi = 90°$, the two top screen edge locations were analyzed. As shown in Figure 9, moving the patch along the top screen edge changed the contribution of the wave reflected from the keyboard structure, which mainly moved the direction of maximum radiation in the azimuth plane (visible in the three-dimensional "without user" patterns, Figure 17). For the center-top screen location (4A), the human body caused shadowing of up to 15 dB in the approximate azimuth range of 30° to 30° and the elevation range of −100° to 70°, independently of the screen inclination angle, Ψ. For the left-corner location (4B), the shadowed area moved in azimuth to 30° to 50°. In this scenario, the radiator was out of the structure's symmetry plane, and shadowing by the user's head was much less pronounced in the vertical-plane pattern (the shadowed region decreased to 100° to 40°). For the center-left screen location (4C), the laptop setup freestanding pattern was significantly different from the top screen location case (4A, 4B). However, the comparison of freestanding and in-situ patterns showed similar human-blocking effects as for the left-corner top screen edge location (4B). The main difference was a further expansion of the horizontal shadow zone to 30° to 60°. Due to the lowering of the illumination source, the shadow of the user's right arm was more pronounced in the horizontal-plane pattern.

In Step 2, the radiation-pattern degradation of middle-screen top-mounted antennas were compared for different ISM 2.4 GHz radiating elements [34]: the sleeve dipole, inverted-F antenna, simple patch, omnidirectional wrapped-microstrip antenna, and back-to-back E-shaped patch (see Figure 18). As could be observed (Figure 18, column 1), except for the simple patch, all antennas operating without the user had reasonably uniform horizontal-plane coverage. The sleeve dipole and the omnidirectional wrapped-microstrip antenna were closer to omnidirectional. As previously shown in Section 3.1, the freestanding radiation patterns of all the top-screen-mounted laptop antennas (see Figure 9 for comparison) were significantly affected by the keyboard. The keyboard-blocking effect was clearly visible in the elevation (V-plane) range of −90° to 0°, whereas the power reflected from the keyboard surface created an interference pattern in the elevation range of 0° to 90°. The far-field radiation pattern of a simple patch was almost not affected by the keyboard, due to the very small amount of energy radiated to the front-screen hemisphere.

For each antenna element considered, the presence of the laptop user caused backward-radiation blocking (up to 25 dB for the sleeve dipole, and up to 15 dB for the other antennas), visible in the azimuth (H-plane) range of −30° to 30°, and in the elevation range of −100° to 70°. For the sleeve dipole, the azimuth span shadowed by the user was slightly smaller than for the other antenna types, because this design had the highest antenna location (at the height of the user's neck).

In Step 3, the effects of the human's presence were compared for internal and externally mounted inverted-F antennas (Figure 19). The far-field gain pattern of the laptop setup (without the user) for the antenna in the front keyboard position (1B) is presented in the first row of the figure. The screen-shadowing effect is visible in the horizontal cut in the azimuth range of 90° to 150°. The enhanced radiation in the direction of the user's right arm (see the three-dimensional plot) was caused by the corner reflector

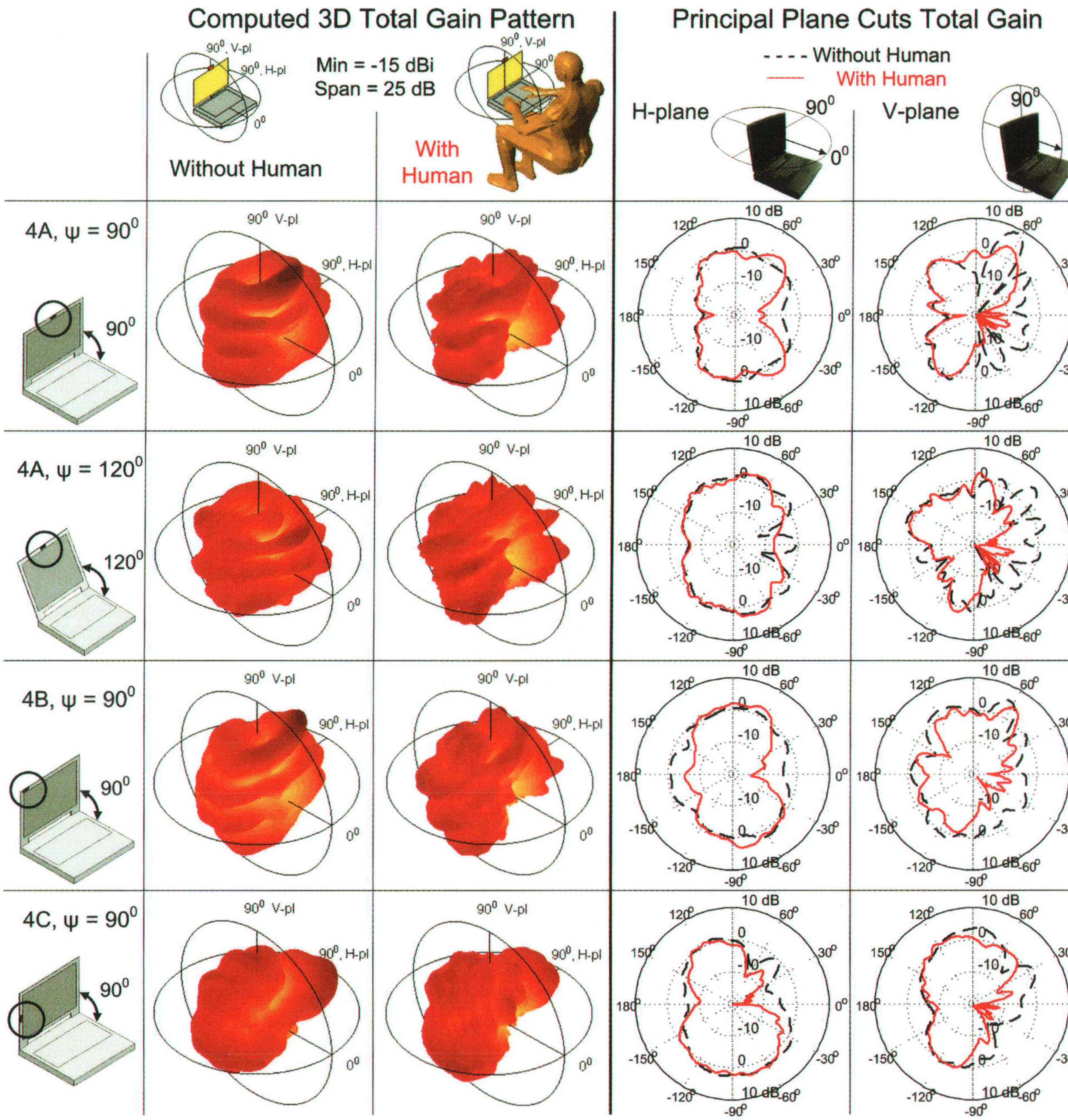

Figure 17. The effects of the laptop's user on the 2.44 GHz far-field gain patterns of a back-to-back E-shaped antenna for different patch locations and laptop-opening angles (Step 1 of the analysis).

formed by the screen and keyboard, as presented in Section 3.2, Figure 13. The presence of the typing user drastically changed the radiation from the antenna (second column). The upward radiation was blocked by the user's wrist (which, in this antenna location, was over the antenna element) by as much as 10 dB (see the V-plane cut). A strong blocking effect by the torso (up to −15 dB) was visible in the −10° to 50° azimuth range. In the non-typing position (third column), there was no blocking effect of the upward radiation (the hand did not cover the antenna), but the blocking of backward radiation slightly increased (as the arms were relaxed along the trunk).

The computational results for the antenna located at the back keyboard position (1A) are shown in Figure 19, second row. Effects similar to (1B) were observed, with the only major difference being in the upward radiation blockage. For this antenna position, the user's hand did not cover the inverted-F antenna element; therefore, in the typing position, it caused almost no upward shadowing.

The comparison between scenarios for the PCMCIA integrated antenna (Figure 19, rows 1 and 2) and the screen-integrated antenna (rows 3, already analyzed in Step 2) clearly showed a significantly stronger user interaction for the external antennas. This also resulted in lower radiation efficiencies (Section 4.4), and significantly higher SAR values for the PCMCIA antennas (Section 4.5). Moreover, contrary to the case for the screen-integrated antennas, the user's posture had a strong influence on the EM interaction with PCMCIA-mounted radiators (compare the second and third columns of Figure 19).

In all the analyzed scenarios (Steps 1, 2, and 3), the human tissue partially reflected and partially absorbed the incident electromagnetic waves. The reflected component contributed to the far-field radiation pattern, and due to interference with the primary source (defined here as the entire laptop structure), was visible in the form of ripple. The absorbed component led to reduction of the antenna-user setup radiation efficiency, as discussed in Section 4.4.

4.4 User Effects on Radiation Efficiency

In the numerical simulations, the structures of the antenna element and laptop housing were modeled as composed solely of PECs and lossless dielectrics. The entire power absorbed by the system, P_{abs}, therefore corresponded to the human body, only. The radiation efficiency of the laptop-user system is defined as

$$\eta_r = \frac{P_{rad}}{P_{rad} + P_{abs}} = \frac{P_{rad}}{P_{acc}} , \qquad (1)$$

where P_{rad} is the power radiated to the far-field region, P_{acc} is the antenna-accepted power, and P_{abs} is the power absorbed by the human body. As defined, this parameter does not take into account the antenna input-mismatch loss.

The back-to-back E-shaped antenna's radiation efficiency, calculated according to Equation (1), for all Step 1 scenarios, is presented in Figure 20. For the top-edge locations, the total power absorbed by the typing human was practically the same, and never exceeded 7% of the antenna-accepted power. The highest amount of energy absorbed by the human tissues was obtained for the side-mounted antenna, where the distance between the user's hand and the patch was the smallest. In this case, the radiation efficiency dropped down to 87.9%, which (as will be shown later) was still 10% higher than the highest efficiency of a PCMCIA-card-mounted inverted-F antenna.

The comparison between different antennas located in the middle top screen (Step 2 of the analysis) is presented in Figure 21. It can be seen that the radiation efficiency of the back-to-back E-shaped antenna was the second highest (94.2%, after 99.3% for the simple patch, which practically did not radiate towards the user's body). The lowest radiation efficiency (86.7%) was obtained for the sleeve dipole, which, in spite of very low peak SAR (see Section 4.5), illuminated the human face, torso, and arms most uniformly, leading to higher energy loss.

Results for PCMCIA-mounted and internal inverted-F antenna elements (Step 3) are presented in Figure 22. Contrary to screen-mounted antennas, in the PCMCIA-card antennas, the user's posture had a key effect on the EM human interaction. It was clear that the worst radiation efficiency was obtained for the antenna in the front keyboard location (1B), when the user was in the typing position. In this case, where the user's wrist covered the inverted-F antenna element, the human tissue absorbed 55.8% of the energy. The amount of energy absorbed by the operator was significantly reduced when the hands were taken away from the keyboard (a non-typing user absorbed 16.2%). In spite of the comparably small minimum distance between the antenna and the arm in the back keyboard location (1A compared with 1B), the energy absorption was only 23% (compared with 56% for the front keyboard scenario). The improved antenna efficiency was caused by placement of the user's hand over the antenna's ground plane (constituted by the keyboard), where near fields were much less intense than over the inverted-F antenna slot.

The highest PCMCIA-card-mounted antenna efficiency obtained for user typing positions was 10% lower than the lowest radiation efficiency of the screen-integrated antennas, analyzed in Step 1 (Figure 20) and Step 2 (Figure 21).

4.5 Antenna Effects on the User (SAR)

Electromagnetic energy absorbed by the human body can potentially present a health risk, and there has been a generalized and persistent public concern about it. Therefore, it is necessary to quantify, if not minimize, this phenomenon. The maximum exposure of human tissue to electromagnetic fields has been defined in terms of Specific Absorption Rate (SAR). In Europe, the maximum allowable SAR (averaged over 10 g of tissue) is 2 W/kg [38]. The laptop user's SAR, for all the investigated scenarios, was evaluated by considering an antenna-accepted power of $P_{acc} = 1$ W (peak). Figures 20, 21, and 22 present the 10 g averaged SAR distributions on the human body's surface, and the peak three-dimensional SAR values.

Results of the Step 1 analysis are presented in Figure 20. The distribution of SAR in the human body depends on the antenna's location. For all the investigated typing-user scenarios, the highest peak SAR values occurred in the user's hands, and reached a maximum of 0.4 W/kg for the side patch location. Changing the patch from the center to the left-corner top screen edge caused a shift in the azimuth of the freestanding laptop maximum radiation (as stated in Section 3.1, Figure 9). This affected the human illumination: for the left-corner location, the area of maximum SAR in the

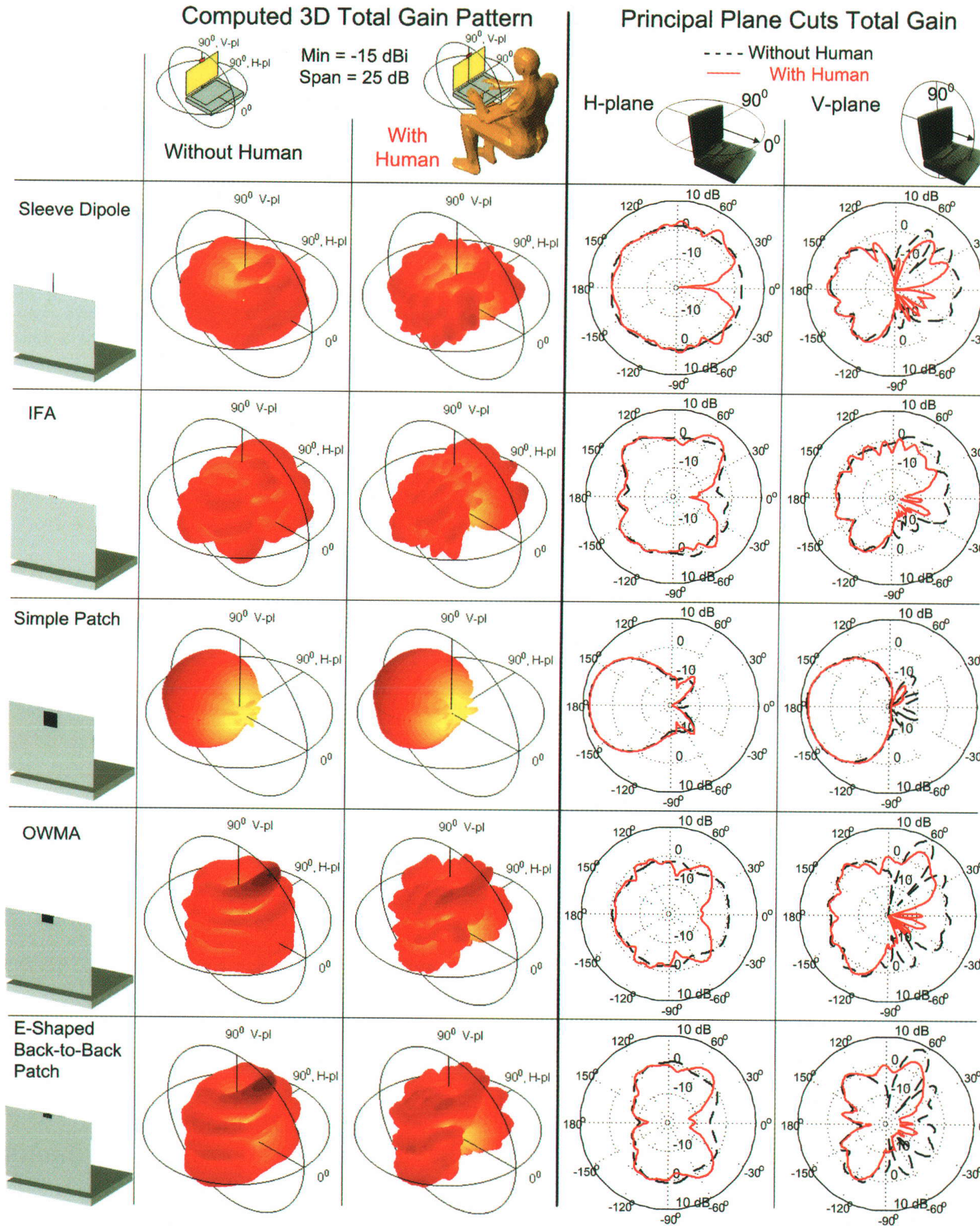

Figure 18. The effects of the laptop's user on the 2.44 GHz far-field gain patterns of different laptop antennas mounted in the top screen location (Step 2 of the analysis).

torso was shifted towards the right arm. For the side-antenna location, the keyboard did not protect the legs from the antenna's illumination, which led to high SAR values in the knees. It can also be seen that the SAR distribution was a function of the screen-opening angle. As the location of minima and maxima in the laptop freestanding far-field radiation pattern were strongly dependent on Ψ (Section 3.1, Figure 9), the location of the areas with higher and lower absorption also changed with the screen position. Bending the screen backward increased the illumination of the user's knees, not covered by the keyboard for $\Psi > 90°$.

The results of the Step 2 analysis are presented in Figure 21. It can be seen that the SAR distribution varied for different antenna types, reaching the lowest values for the simple patch (which practically did not radiate in the front screen hemisphere). For the sleeve dipole, the SAR in the user's upper-body part had the most uniform distribution, leading to the highest total absorbed power (as mentioned in Section 4.4). Due to the radiator's proximity, the peak SAR values occurred in the user's palms for all the antennas. However, even for the worst scenario (the E-shaped back-to-back antenna), they were almost 20 times lower than the 2 W/kg safety limit defined by the guidelines [38].

Results of the last (Step 3) analysis are presented in Figure 22. As expected, the highest SAR values occurred in tissues near the antenna element: the hands of the typing user. The maximum three-dimensional SAR of 2.74 W/kg occurred in the wrist covering the inverted-F antenna in the front keyboard location (1B), which was almost seven times higher than the corresponding peak SAR for screen-integrated antennas (see Steps 1 and 2). Lower values of hand SAR were obtained in the typing position for the back card antenna location (1A). Significant SAR values appeared on the user's legs under the antenna for the keyboard locations considered. It was interesting to note that the leg illumination was higher in the typing position, as part of the energy was reflected by the arm and redirected to the leg. For the screen top location (4A), the illumination of the legs was very low as compared to the PCMCIA locations, due to keyboard shielding. It is also worth mentioning that for the antenna keyboard locations, the illumination of the face was reduced in the typing position, as the hands partially blocked the upward radiation.

It should be noted that all given values of SAR were normalized to 1 W peak antenna output power, while typically a WLAN antenna radiates only about 10 mW. In a real operating system, the maximum value of 0.027 W/kg SAR (user typing position, PCMCIA antenna in 1B location) is therefore expected, which is almost a hundred times below the European standard safety limit [38]. However, it should be noted that other wireless laptop interfaces, such as cellular modems or WiMAX radios, can work with much higher power levels; also, tissue properties are frequency dependent [37]. Modern laptop computers may integrate several antenna elements (see Appendix 3), which, during simultaneous operation, may lead to higher SAR levels. Finally, the simplified homogenous human model does not take into account the different electromagnetic properties of different human tissues, and provides only an estimation of the absorbed energy.

5. Conclusions

This feature article has presented an overview of all the important steps of a successful laptop-antenna subsystem development: radiator design, integration issues, and a discussion of electromagnetic human interaction. The first main contribution was a comprehensive and unified summary of wrapped microstrip antennas for laptops, recently developed at the Instituto de Telecomunicações/Instituto Superior Técnico, Portugal, in cooperation with the ARAM Laboratory, UCLA. Single- and dual-band antennas designed according to a new proposed concept were conformably wrapped around the laptop's screen edge, and, in spite of integration into the laptop's electrically large metallic structure, they presented a quasi-omnidirectional (horizontal-plane) radiation pattern. In addition to the new design concept introduced – an omnidirectional wrapped-microstrip antenna (OWMA) – the most common commercially available internal and external laptop-antenna structures have been analyzed, giving a broader overview of laptop-antenna design approaches.

The second part of the paper extensively discussed laptop-antenna housing aspects. The integration effects were analyzed both for omnidirectional wrapped-microstrip antenna elements, as well as for representative examples of internal and external commercially available antennas. Several laptop-antenna locations and screen-opening angles were considered. It has been shown that the laptop's housing and the antenna's location play key roles in the antenna's performance.

The last major contribution was a general analysis of electromagnetic human interaction with laptop antennas, from the viewpoint of antenna-performance degradation and human-tissue illumination. This study was performed in a systematic fashion for various classes of internal and external antenna elements, several antenna locations, and for several screen-opening angles.

The results clearly showed that the antenna's performance is affected by the laptop's structure and by the user's presence. Therefore, in a rigorous approach, antenna, laptop, and user have to be analyzed as a whole.

6. Acknowledgements

The authors would like to thank Dr. David W. Browne and Prof. Michael P. Fitz for their cooperation in the design of MIMO arrays and in extensive system-level evaluation of arrays.

This work was supported financially by the Instituto de Telecomunicações and the Portuguese Research Council (FCT), and was carried out at Instituto de Telecomunicações and the University of California, Los Angeles.

7. Appendix 1: Commercial (External and Internal) Laptop Antennas

The initial implementations integrating wireless subsystems into laptops used PC cards inserted into slots. The retractable or internal antenna was located in the extreme part of the card (PCMCIA or USB dongle), protruding from the side of the portable computer (locations 1A and 1B in Figure 6). With the use of wireless cards, users can easily add functionality to their laptops, which make those solutions still very popular. As wireless technology becomes prevalent and less expensive, manufacturers are moving away from PC cards, in favor of integrated implementations

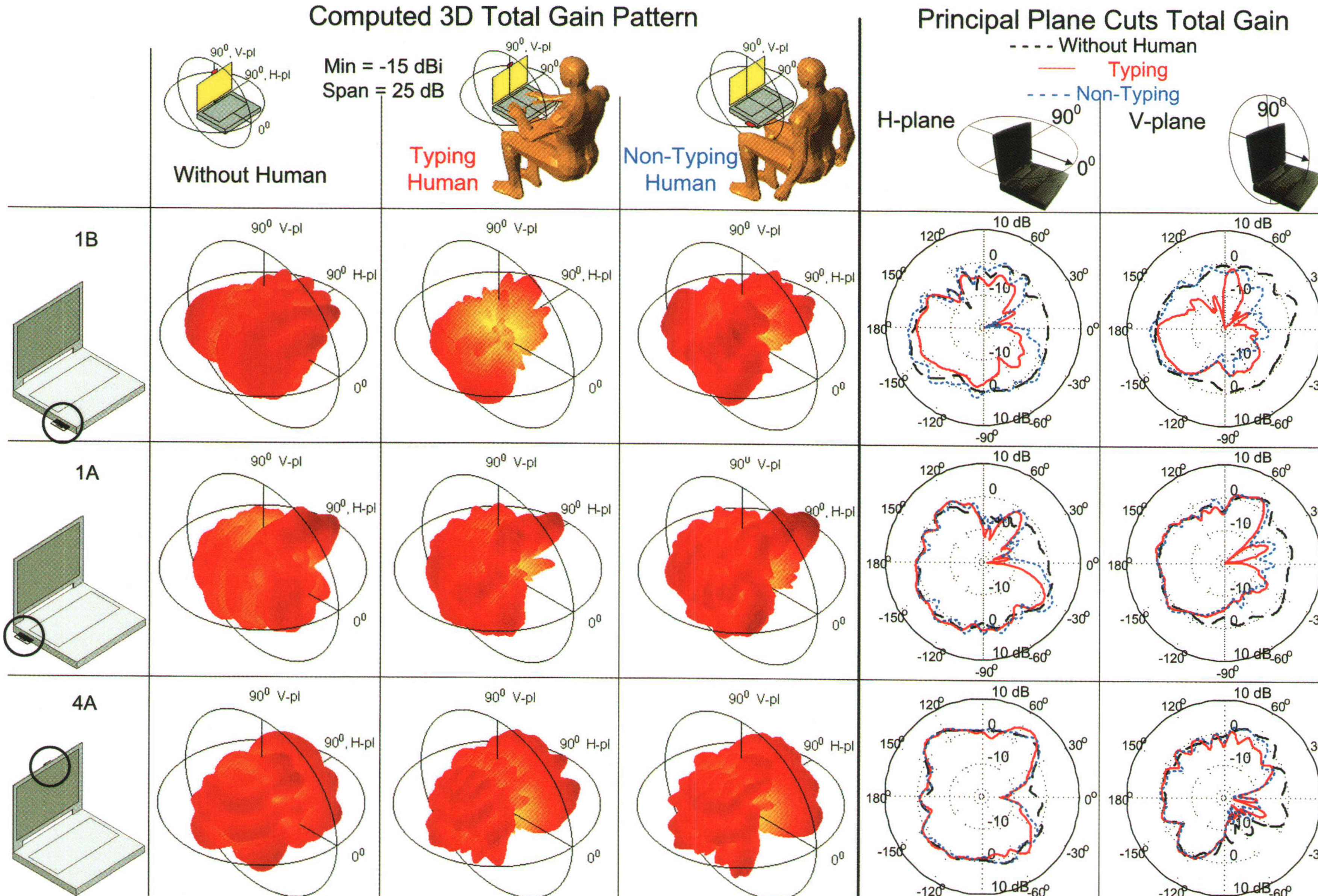

Figure 19. The effects of the laptop's user on the 2.44 GHz far-field gain patterns of an inverted-F antenna (IFA) element integrated into the screen (4A) and PMCIA card (1A, 1B) (Step 3 of the analysis).

[10]. This trend goes with a general tendency of making portable computers more compact and sleek: all the external and protruding components are being eliminated, in order to facilitate the laptop's use and to reduce the risk of physical breakage.

In this appendix, the most-common antenna configurations used for laptop plug-in and build-in interfaces are described. In many practical applications, the outlined structures are modified according to particular design constraints. The characteristics of an antenna integrated into a laptop system, both in the case of a plug-in card and of an internal antenna, depend strongly on its location, the distance to nearby components, and materials covering the device, as described in Section 3. The representative locations of different laptop antenna types are listed in Figure 6. For simplicity, and due to physical symmetry, only left-side locations are shown.

The sleeve dipole (Figure 23a) has been used in the initial implementations of laptop wireless cards. Its radiating structure is an asymmetric dipole made of conductors of different diameters and slightly different lengths. The thinner conductor – typically, the extension of the coaxial-feeding inner conductor – must have an appropriate length to achieve a good antenna impedance match in the band of operation. The large-diameter conductor sleeve must provide effective choking of the RF currents at its own open end, and also at one-half of the radiating dipole [39]. An ISM 2.4 GHz coaxial-sleeve dipole was used in this paper for the laptop housing study (Section 3.2) and for the electromagnetic human-interaction study (Section 4). A sleeve dipole can be realized in a planar structure as a strip sleeve dipole. Multi-band strip sleeve dipoles have been reported in [6] and [40].

An inverted-F antenna (IFA) structure is shown in Figure 23b. The quarter-wavelength arm is parallel to the ground-plane's edge, which makes the inverted-F antenna easy to integrate within a limited space. Essentially, it is half of the traditional $\lambda/2$ slot antenna, and their mechanisms of operation are analogous. By moving the feeding stub from the shorting stub to the open-slot end, the inverted-F antenna's input impedance changes from very low to very high values. The feeding point is selected in order to obtain an impedance match to the 50 Ω line. The slot height is calculated according to the antenna's required frequency band [41]. For a 3.4% wide ISM 2.4 GHz band, the slot height ranges between five and six millimeters. The inverted-F antenna can be printed on the protruding part of the PCMCIA board [42], and fed by a coplanar waveguide (locations 1A and 1B, Figure 6). The inverted-F antenna element is also widely used as an internal antenna, integrated along the laptop's screen edge [10]. A screen-integrated ISM 2.4 GHz inverted-F antenna was used in this paper for the laptop-housing study (Section 3.2). The single-band flat-plate antenna [43] has a configuration similar to the inverted-F antenna. It can also be cut from a thin metal sheet, and fed by a miniaturized coaxial cable. The dual-band flat-plate antenna's arm may have a more convoluted shape: two examples of integration into a laptop screen rim were described in [44] and [45].

The slot antenna can be considered to be a loaded version of the inverted-F antenna, where the load is a quarter-wavelength stub. Since the quarter-wavelength stub itself is a narrowband system, the slot antenna has a narrow bandwidth [10]. Classical slot antennas, due to bigger dimensions than inverted-F antennas, are implemented as internal laptop antennas [11]. In wireless plug-in interfaces, tapered meander-slot antennas can be used [46].

The chip antenna is a very compact surface-mountable device (Figure 23c). It comprises a high-permittivity dielectric body ($\varepsilon_r > 7$) with an embedded meandering metal line. In many practical implementations, low-temperature co-fired ceramic (LTCC) technology is used: conducting strips are printed on different ceramic layers, and are connected by metal via posts, forming a continuous three-dimensional path. The path's shape depends on the application and required miniaturization, and may have the form of a helix [47], a meander [47], or a spiral [48]. Thanks to the very small size and the ability to be surface mounted, chip antennas are used in laptop wireless interfaces, both in external plug-in devices and as built-in antennas. Due to the high permittivity of the ceramic substrates, the electromagnetic field is concentrated in this

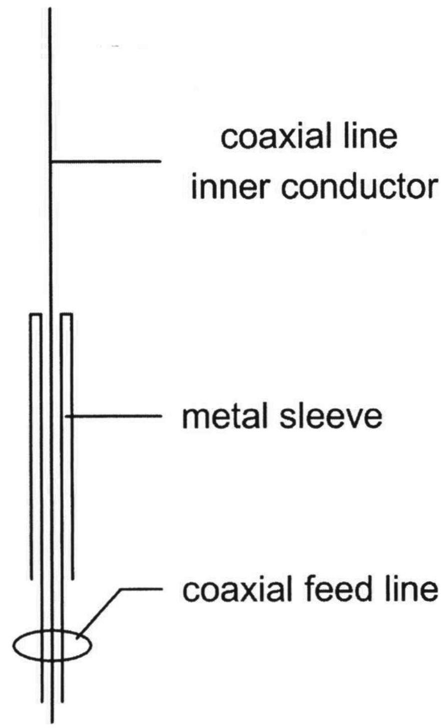

Figure 23a. A representative example of a commercially available laptop antenna: a sleeve dipole.

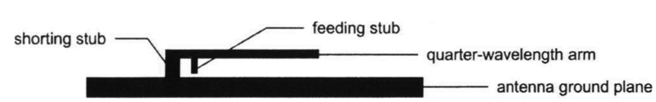

Figure 23b. A representative example of a commercially available laptop antenna: an inverted-F antenna (IFA).

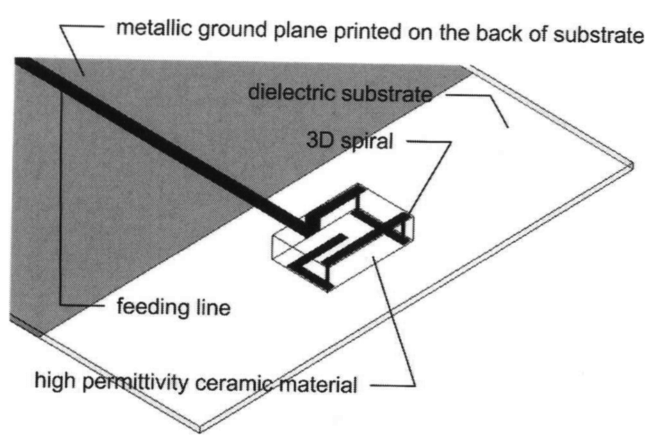

Figure 23c. A representative example of a commercially available laptop antenna: a chip antenna.

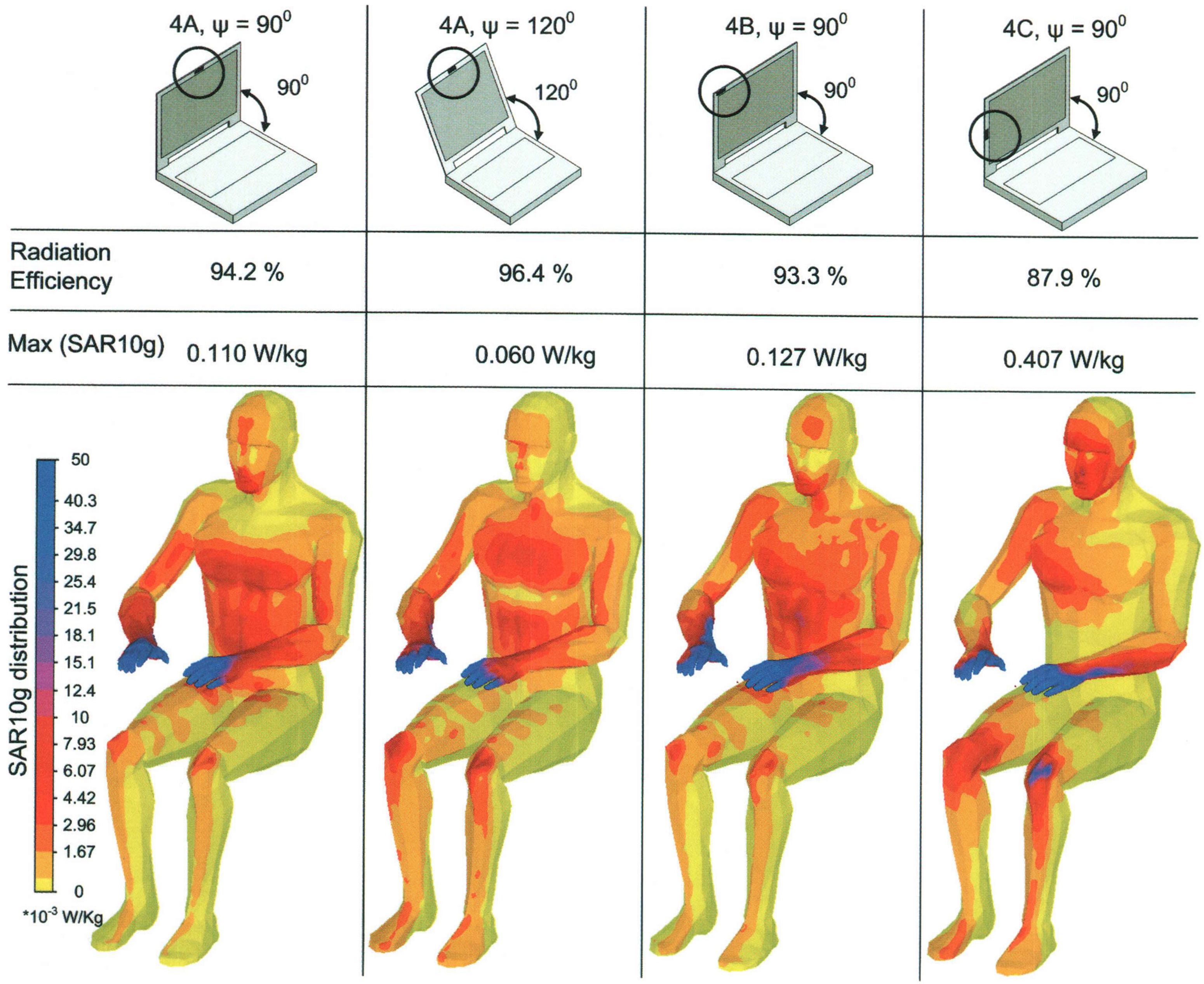

Figure 20. The absorption of electromagnetic energy in human tissue: the resulting antenna radiation efficiencies and SARs in the operator's body at 2.44 GHz for different screen-integrated antenna locations and screen-opening angles.

low-loss part of the radiator. A chip antenna can therefore achieve an acceptable radiation efficiency even when mounted on a high-loss circuit board.

8. Appendix 2: Fabrication and Measurement of Wrapped Microstrip Laptop Antennas

All the simulations of microstrip antennas and commercial internal and external radiators presented used a simplified laptop model, consisting of:

- A keyboard base: a 295×260×25 [mm^3] PEC box;
- A lid: a 245×260×5 [mm^3] PEC box, inclined by Ψ to the keyboard base;
- A PCMCIA card: a 102×50×5 [mm^3] PEC box (for simulation of external antennas).

Wrapped microstrip antenna elements use the metallic display layers as a natural ground plane. For the sake of prototyping, a 14 in TFT panel has been modeled as a [295×225×1] mm^3 (W×H×T) brass plate. Front and back patch sections were printed on 62 mils thick Rogers DuroidTM 5880 ($\varepsilon_r = 2.2$) dielectric substrates. Additionally, thin air gaps were introduced between layers, in order to increase the (impedance) bandwidth and to facilitate the feeding of the antenna. As an example, the 2.4/5.2 GHz back-to-back E-shaped antenna layers are shown in Figure 24a. The patch connecting section was made from a thin metal plate, and welded to the structure. The antenna prototype was fed by a microstrip inverted line, printed on the internal side of the back dielectric substrate. The feeding line is shown in Figure 24b. To assure sufficient proximity coupling, the line went underneath the back patch section. The antenna input impedance could be tuned by adjusting the length of the buried line underneath the patch; a short tuning stub assured good matching in both operating bands.

In a commercial implementation, a wrapped microstrip patch can be printed on the backside of the screen's plastic casing and fed by a miniature coaxial cable, instead of using additional substrates.

During the antenna-housing effects measurements, the antenna prototypes were attached to a real Toshiba Satellite 4200 PRO keyboard chassis (see Figure 11b). The very good agreement obtained between simulation and measurement results (see Section 3.1) validated the simplified laptop model used in the numerical simulations.

Antenna input matching was measured with a network analyzer. Due to the relatively large electrical size of the laptop, the radiation-pattern measurements were performed in the near-field region. The antenna prototypes were measured in UCLA's spherical near-field range, as shown in Figure 11. The distance between the antenna under test and the probe was 1.52 m, and the anechoic chamber measured 6.1×2.7×2.6 m^3. NSI2000 software was used to evaluate the far-field radiation pattern in the entire angular range. The antenna setup was attached to the positioner by the keyboard-base's bottom side (Figure 11b). The highest measurement error caused by the shadowing of the positioner for the antenna under test occurred for angles corresponding to the laptop's bottom side, which is of less importance for a typical wireless scenario. It was found that due to the relatively large electrical size of the radiating structure, the laptop setup's feeding cable practically did not disturb the measurements; therefore, there was no need for using choking ferrites. Parts of the measurements in the 2.4 GHz band were repeated in the far-field range of the Instituto Superior Técnico, Lisbon, Portugal. Excellent agreement was obtained.

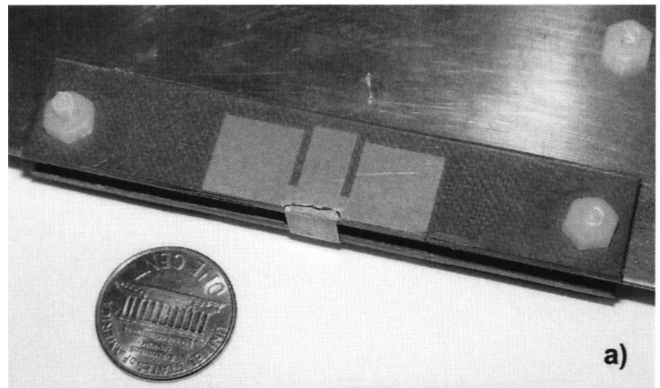

Figure 24a. The antenna prototype: the antenna element's front side (a US penny was used as a reference).

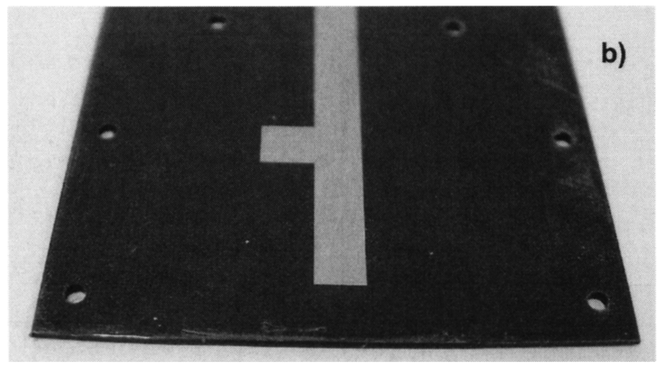

Figure 24b. The antenna prototype: the microstrip inverted line with the tuning stub, printed on the internal side of the back substrate.

9. Appendix 3: Multi-Antenna System for MIMO-Enabled Laptops

The growing demands of high spectrum efficiency and wireless-link reliability call for recent achievements in diversity [49], smart antennas, and multiple-input multiple-output (MIMO) techniques [50]. Integrated multiple-element antenna arrangements are therefore highly beneficial in laptop applications, and are expected to become a standard in the near future. The optimization of these arrangements incorporates aspects of antenna-element design (see Section 2 and Appendix 1) and integration (see Section 3), as well as multi-antenna topology design issues. The multi-antenna design paradigm differs for the diversity, smart-antenna, and MIMO concepts [51]. This section briefly overviews multi-antenna arrangements for MIMO-enabled laptops.

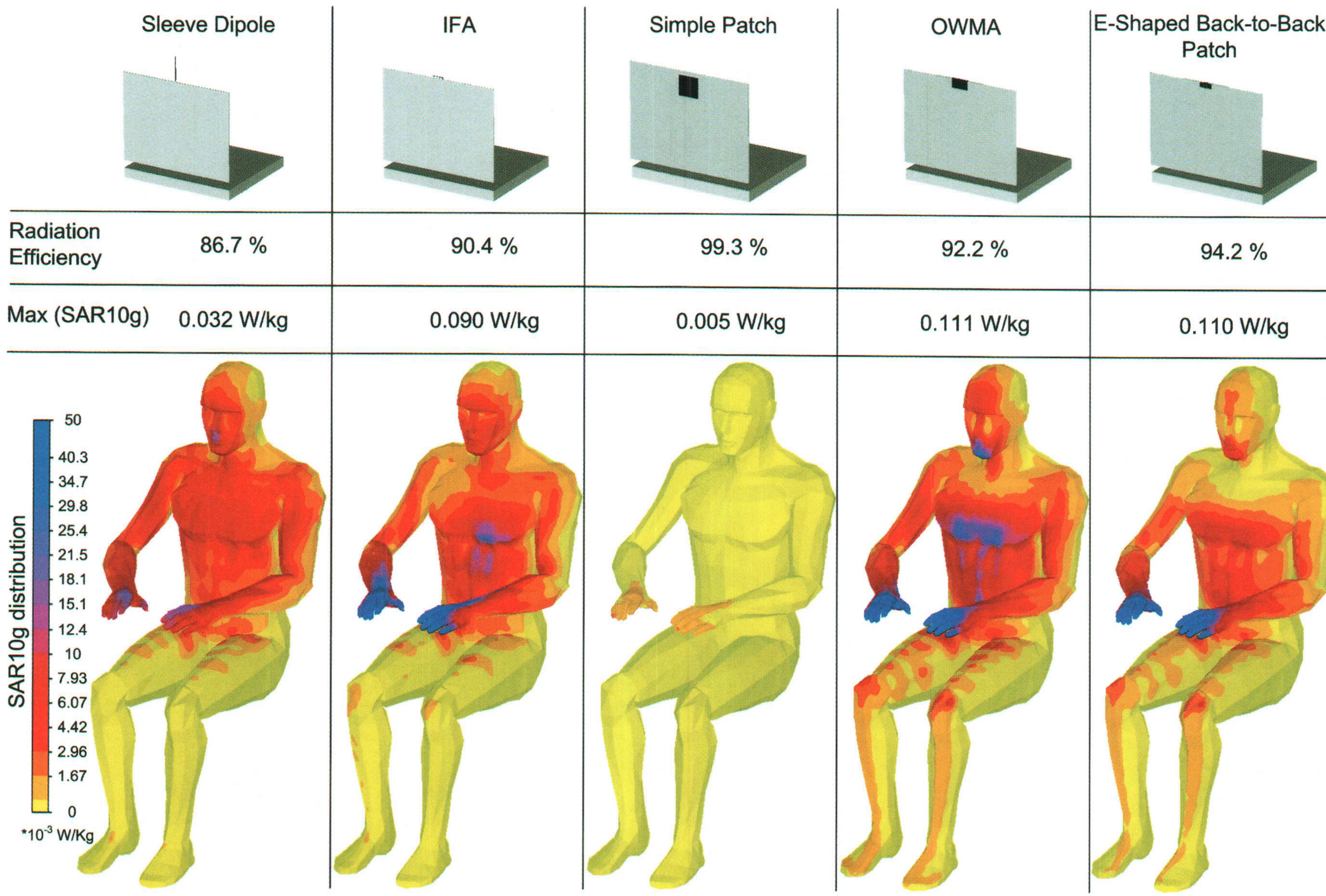

Figure 21. The absorption of electromagnetic energy in human tissue: the resulting antenna radiation efficiencies and SARs in the operator's body at 2.44 GHz for different antenna types integrated in the middle top screen position.

From the wireless-system-operation point of view, the design of a MIMO mobile unit is evaluated according to system-level performance measures, e.g., capacity and signal-to-noise ratio (SNR). The MIMO array interfaces with the MIMO channel. Its antenna-level parameters (namely, input matching, mutual coupling, radiation efficiency, and radiation patterns) should therefore be chosen in order to maximize the achievable system-level performance by maximum utilization of the multipath. It has been suggested [51] that an optimal MIMO array should consist of omnidirectional elements with high radiation efficiency and low mutual coupling between ports. Moreover, recent experimental work has confirmed that an array of omnidirectional elements outperforms a sector array in a wide range of indoor scenarios [52].

This observation has encouraged authors to design novel MIMO arrays for laptops based on omnidirectional wrapped-

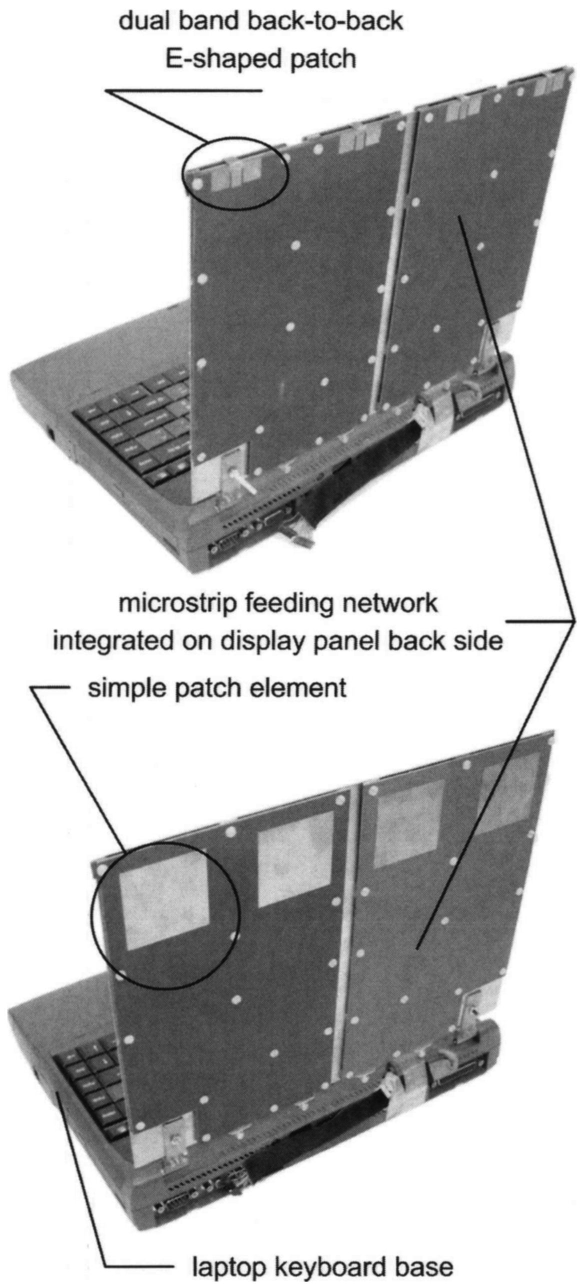

Figure 25. Four-element linear arrays attached to a commercial laptop chassis: a back-to-back E-shaped patch array (top) and a simple patch array (bottom).

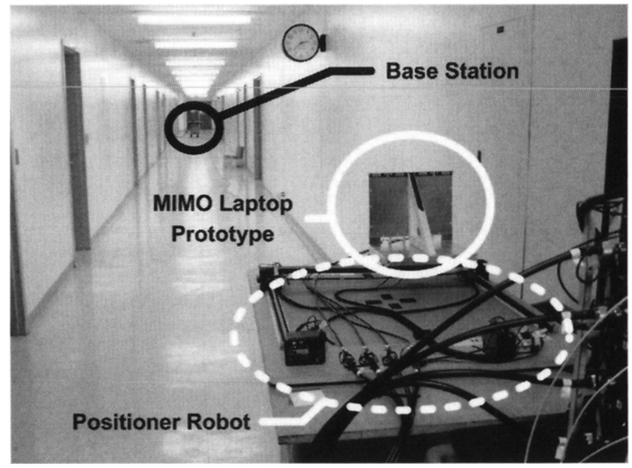

Figure 26a. The MIMO experimental setup, showing the base station and the MIMO laptop prototype.

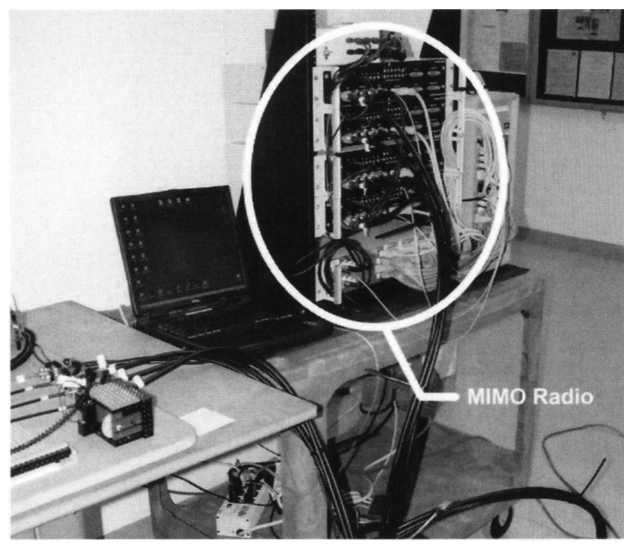

Figure 26b. The MIMO experimental setup, showing the MIMO radio.

microstrip antennas [53, 54] and back-to-back E-shaped elements [16]. These elements are inherently quasi-omnidirectional, and due to low profiles, posses low mutual coupling. In [16], the design and laptop integration of two linear four-element laptop integrated MIMO arrays was described: (i) a linear array of 2.4/5.2 GHz back-to-back E-shaped elements, and (ii) a linear array of simple 2.4 GHz patch elements (see Figure 25). In the ISM 2.4 GHz band, those arrays are characterized by a very similar scattering matrix and similar radiation efficiencies, while having significantly different element radiation patterns (for a comparison of the radiation patterns, see Figure 2). The system-level performance of those two arrays was evaluated with the aid of a true MIMO test-bed (Figure 26) in a wide range of line-of-sight and non-line-of-sight indoor scenarios [55]. It was shown that in spite of the laptop's housing effects (see Section 3), the array of back-to-back E-shaped elements outperformed the classical array in terms of MIMO capacity.

Design and system-level measurements of very compact two- and four-element arrays of a triple-band PIFA (planar inverted-F antenna), to be integrated into a laptop PCMCIA card, were reported in [51]. However, this study did not take into account a realistic laptop housing model.

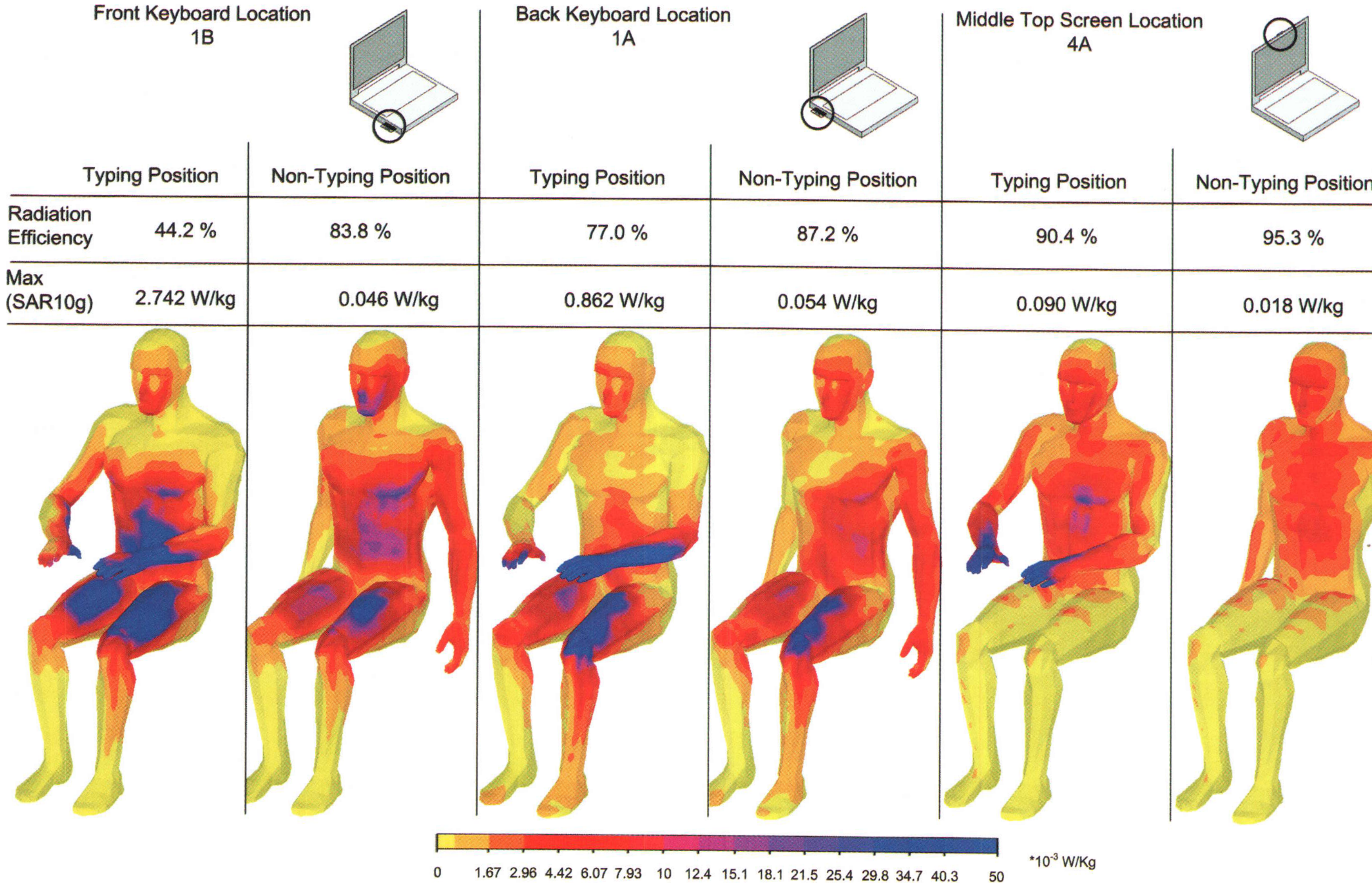

Figure 22. The absorption of electromagnetic energy in human tissue: the resulting antenna radiation efficiencies and SARs in the operator's body at 2.44 GHz for different inverted-F antenna (IFA) element locations.

10. References

1. Consumer Behavior Report, July 2006, "Wireless Lifestyle Trends," available at https://mr.pricegrabber.com/july_2006_consumer_behavior_report.pdf.

2. Ezra Goldman, "From Mobility Devices to Connectivity Devices: Rethinking the Role of Space in a Networked World," *IEEE Pervasive Computing*, **6**, 3, July-September 2007, pp. 12-14.

3. J. Bray and C. Sturman, *Bluetooth: Connect Without Cables*, Englewood Cliffs, NJ, Prentice-Hall, Inc., 2000.

4. J. Geier, *Wireless LANs: Implementing Interoperable Networks*, Indianapolis, Macmillan Technical Publishing, 1999.

5. B. Razavi, "Gadgets Grab at GHz," *IEEE Spectrum*, **45**, 2, February 2008, pp. 40-45.

6. M. Ali, M. Okoniewski, M. A. Stuchly and S. S. Stuchly, "Dual-Frequency Strip-Sleeve Monopole for Laptop Computers," *IEEE Transactions on Antennas and Propagation*, **AP-47**, 1, February 1999, pp. 317-323.

7. D. Liu, B. Gaucher and T. Hildner, "A Dualband Antenna for WLAN Applications," Proceedings of the IEEE International Workshop on Antenna Technology: Small Antennas and Novel Metamaterials iWAT, Marina Mandarin Singapore, pp. 201–204, March 2005, pp. 201-204.

8. M. Manteghi and Y. Rahmat-Samii, "Novel Compact Tri-Band Two-Element and Four-Element MIMO Antenna Designs," IEEE International Symposium on Antennas and Propagation *Digest*, Albuquerque, NM, USA, July 2006, pp. 4443-4446.

9. D. Liu, and B. Gaucher, "A Triband Antenna for WLAN Applications," IEEE International Symposium on Antennas and Propagation *Digest*, **2**, Columbus, Ohio, USA, June 2003, pp. 18-21.

10. D. Liu, B. P. Gaucher, E. B. Flint, T. W. Studwell, H. Usui and T. J. Beukema, "Developing Integrated Antenna Subsystems for Laptop Computers," *IBM Journal of Research and Development*, **47**, 2/3, March/May 2003, pp. 355-367.

11. R. Bancroft, "A Commercial Perspective on the Development and Integration of an 802.11a/b/g Hiperlan/WLAN Antenna into Laptop Computers," *IEEE Antennas and Propagation Magazine*, **48**, 4, August 2006, pp. 12-18.

12. D. Manteuffel, A. Bahr, D. Heberling, and I. Wolff, "Design Considerations for Integrated Mobile Phone Antennas," Proceedings of the International Conference on Antennas and Propagation (ICAP), **1**, London, UK, April 2001, pp. 252-256.

13. J. Guterman, A. A. Moreira, and C. Peixeiro, "Laptop Screen Inclination Effects on an Integrated Omnidirectional Wrapped Microstrip Antenna," Proceedings of the IST Mobile Communications Summit, Myconos, Greece, June 2006.

14. J. Guterman, Y. Rahmat-Samii, A. A. Moreira and C. Peixeiro, "Radiation Pattern Study of 2.4/5.2 GHz Laptop Internal Antenna: Near Field Spherical Range Measurements and Full Wave Analysis," Proceedings of the International Workshop on Antenna Technology (iWAT), Cambridge, United Kingdom, March 2007.

15. J. Antoniuk, "Integration of Microstrip Patch Antennas into Laptop Computers," Graduation Report, Instituto Superior Técnico, Lisbon, October 2003.

16. J. Guterman, D. W. Browne, Y. Rahmat-Samii, A. A. Moreira and C. Peixeiro, "Design of Integrated Antenna Arrays for MIMO Enabled Laptops," IEEE International Symposium on Antennas and Propagation *Digest*, Honolulu, Hawaii USA, June 2007.

17. J. Antoniuk, J. Guterman, A. A. Moreira, and C. Peixeiro, "Location of Patch Antennas for Wireless Applications in Laptops," Proceedings of the Conference on Telecommunications (ConfTele), Tomar, Portugal, April 2005.

18. J. Antoniuk, A. A. Moreira and C. Peixeiro, "L-Bent Omnidirectional Patch Antenna for Wireless Applications in Laptop Computers," IEEE International Symposium on Antennas and Propagation *Digest*, **4A**, Washington DC, USA, July 2005, pp. 355-358.

19. J. Guterman, A. A. Moreira, and C. Peixeiro, "Omnidirectional Wrapped Microstrip Antenna for WLAN Applications in Laptop Computers," IEEE International Symposium on Antennas and Propagation and USNC/URSI National Radio Science Meeting, **3B**, Washington, DC, July 2005, pp. 301-304.

20. J. Zurcher and F. E. Gardiol, *Broadband Patch Antennas*, Norwood, MA, Artech House, 1995.

21. J. Guterman, Y. Rahmat-Samii, A. A. Moreira and C. Peixeiro, "Quasi-Omnidirectional Dual-Band Back-to-Back E-shaped Patch Antenna for Laptop Applications," *Electronics Letters*, **42**, 15, July 2006, pp. 845-847.

22. F. Yang, X-X. Zhang, X. Ye, and Y. Rahmat-Samii, "Wide-Band E-Shaped Patch Antennas for Wireless Communications," *IEEE Transactions on Antennas Propagation*, **AP-49**, 7, July 2001, pp. 1094-1100.

23. C. R. Medeiros, J. R. Costa, C. A. Fernandes, and B. M. Kolundzija, "Modelling of a MEMS Reconfigurable Antenna Using WIPL-D," Proceedings of the ESA Antenna Workshop on Multiple Beam and Reconfigurable Antennas, **1**, Noordwijk, Netherlands, April 2007, pp. 369-372.

24. J. Guterman, Y. Rahmat-Samii, A. A. Moreira, and C. Peixeiro, "Quasi-Omnidirectional Back-to-Back E-Shaped Patch Antenna for Dual-Band 2.4/5.2 GHz Laptop Integrated Wireless Interface," Proceedings of the European Conference on Antennas and Propagation EuCAP, Nice, France, November 2006.

25. J. T. Bernhard, "Analysis of Integrated Antenna Positions on a Laptop Computer for Mobile Data Communication," IEEE International Symposium on Antennas and Propagation *Digest*, **4**, Montreal, Canada, July 1997, pp. 2210-2213.

26. F. M. Caimi and G. O'Neill, "Antenna Design for Notebook Computers: Pattern Measurements and Performance Considerations," IEEE International Symposium on Antennas and Propagation *Digest*, **4A**, Washington, DC, July 2005, pp. 247-250.

27. G. H. Huff, J. Feng, S. Zhang; G. Cung and J. T. Bernhard, "Directional Reconfigurable Antennas on Laptop Computers: Simulation, Measurement and Evaluation of Candidate Integration Positions," *IEEE Transactions on Antennas Propagation*, **AP-52**, 12, December 2004, pp. 3220-3227.

 ISSN 1045-9243/2009/$25 ©2009 IEEE

28. J. Guterman, A. A. Moreira, and C. Peixeiro, "Location of Omnidirectional Wrapped Microstrip Antennas in Laptops for Wireless Applications," IEEE International Symposium on Antennas and Propagation *Digest*, Albuquerque, NM, July 2006, pp. 2621-2624.

29. J. Guterman, Y. Rahmat-Samii, A. A. Moreira and C. Peixeiro, "Radiation from Commercially Viable Antennas for PCMCIA Cards Housed in Laptops," 16th IST Mobile and Wireless Communications Summit, Budapest, Hungary, July 2007.

30. M. A. Jensen and Y. Rahmat-Samii, "EM interaction of Handset Antennas and a Human in Personal Communications," *Proceedings of the IEEE*, **83**, 1, January 1995, pp. 7-17.

31. J. Wang and O. Fujimura, "EM Interaction Between a 5GHz Band Antenna Mounted PC and a Realistic Human Body Model," *IEICE Transactions on Communications*, **E88-B**, 6, June 2005, pp. 2604-2608.

32. J. Guterman, A. A. Moreira, C. Peixeiro and Y. Rahmat-Samii, "Laptop Antenna Location Effects on Electromagnetic Human Interaction with E-Shaped Back-to-Back Patch," submitted to ICT Mobile Summit, Stockholm, Sweden, June 2008.

33. J. Guterman, A.A. Moreira, C. Peixeiro and Y. Rahmat-Samii, "Laptop Opening Angle Effects on Electromagnetic Human Interaction with an Integrated E-shaped Back-to-Back Antenna," IEEE International Symposium on Antennas and Propagation, San Diego, USA, July 2008.

34. J. Guterman, A. A. Moreira, C. Peixeiro and Y. Rahmat-Samii, "Comparison Study of Electromagnetic Human Interaction with Various 2.4 GHz Laptop Integrated Antennas," 17th International Conference on Microwaves, Radar and Wireless Communications (MIKON), Wrocław, Poland, May 2008.

35. J. Guterman, A. A. Moreira, C. Peixeiro and Y. Rahmat-Samii, "Electromagnetic Human Interaction with ISM 2.4 GHz Laptop Antennas," Proceedings of the European Conf. on Antennas and Propagation (EuCAP), Edinburgh, United Kingdom, November 2007.

36. M. Clemens and T. Weiland, "Discrete Electromagnetics: Maxwell's Equations Tailored to Numerical Simulations," *International Compumag Society Newsletter (ICS)*, **8**, July 2001, pp. 13-20.

37. An Internet Resource for the Calculation of the Dielectric Properties of Body Tissues in the Frequency Range 10 Hz – 100 GHz, Italian National Research Council, http://niremf.ifac.cnr.it/tissprop/.

38. CENELEC, European Specification ES 59005, "Considerations for the Evaluation of Human Exposure to Electromagnetic Fields (EMFs) from Mobile Telecommunication Equipment (MTE) in the Frequency Range from 30 MHz-6GHz," Ref. No. ES 59005:1998 E, 1998.

39. K. Fujimoto and J. R. James (eds.), *Mobile Antenna Systems Handbook, Second Edition*, Norwood, MA, Artech House Inc., 2001.

40. T. L. Chen, "Multi-Band Printed Sleeve Dipole Antenna," *Electronics Letters*, **39**, 1, January 2003, pp. 14-15.

41. D. Liu, and B. P. Gaucher, "The Inverted-F Antenna Height Effects on Bandwidth," IEEE International Symposium on Antennas and Propagation *Digest*, **2A**, Washington, DC, July 2005, pp. 367-370.

42. C. Soras, M. Karaboikis, G. Tsachtsiris, and V. Makios, "Analysis and Design of an Inverted-F Antenna Printed on a PCMCIA Card for the 2.4 GHz ISM Band," *IEEE Antennas and Propagation Magazine*, **44**, 1, February 2002, pp. 37- 44.

43. C. M. Su and K. L. Wong, "Narrow Flat-Plate Antenna for 2.4 GHz WLAN Operation," *Electronics Letters*, **39**, February 2003, pp. 344-345.

44. K. Wang, L. Chou, and C. Su, "Dual-Band Flat-Plate Antenna with a Shorted Parasitic Element for Laptop Applications," *IEEE Transactions on Antennas and Propagation*, **AP-53**, 1, January 2005, pp. 539-544.

45. T. Ito, H. Moriyasu and M. Matsui, "A Small Antenna For Laptop Applications," Proceedings of the IEEE International Workshop on Antenna Technology Small Antennas and Novel Metamaterials (iWAT), New York, USA, March 2006, pp. 233-236.

46. C. M. Allen, A. Z. Elsherbeni, C. E. Smith, C-W. P. Huang and K-F. Lee, "Tapered Meander Slot Antenna for Dual Band Personal Wireless Communication Systems," *Microwave and Optical Technology Letters*, **36**, 5, March 2003, pp. 381-385.

47. K.-L. Wong, *Planar Antennas for Wireless Communications*, New York, John Wiley & Sons, 2003.

48. C. L. Tang, "2.4/5.2 GHz Dual-band Chip Antenna for WLAN Application," IEEE International Symposium on Antennas and Propagation *Digest*, **1A**, Albuquerque, NM, June 2006, pp. 454-457.

49. R. G. Vaughan and J. B. Andersen, "Antenna Diversity in Mobile Communications," *IEEE Transactions on Vehicular Technology*, **36**, 4, November 1987, pp. 149-172.

50. M. A. Jensen and J. W. Wallace, "A Review of Antennas and Propagation for MIMO Wireless Communications," *IEEE Transactions on Antennas and Propagation*, **AP-52**, 11, November 2004, pp. 2810-2824.

51. D. W. Browne, M. Manteghi, M. P. Fitz and Y. Rahmat-Samii, "Experiments with Compact Antenna Arrays for MIMO Radio Communications," *IEEE Transactions on Antennas and Propagation*, **AP-54**, 11, November 2006, pp. 3239-3250.

52. D. W. Browne, J. Guterman, M. P. Fitz and Y. Rahmat-Samii, "Experimental Validation of Capacity Preserving Design for MIMO Arrays (Invited Paper)," Proceedings of the International Workshop on Antenna Technology, Cambridge, 2007.

53. J. Guterman, A. A. Moreira, and C. Peixeiro, "Omnidirectional Wrapped Microstrip Antennas for MIMO Linear Arrangements in Laptops," IEEE International Symposium on Antennas and Propagation *Digest*, Albuquerque, NM, July 2006, pp. 2625-2628.

54. J. Guterman, A. A. Moreira, and C. Peixeiro, "Multi-Element Omnidirectional Wrapped Microstrip Antenna for MIMO Laptop Integrated Wireless Interface," Proceedings of the European

Conference on Antennas and Propagation (EuCAP), Nice, France, November 2006.

55. David W. Browne, Jerzy Guterman, Yahya Rahmat-Samii, and Michael P. Fitz "Performance of Integrated Antenna Arrays for MIMO Enabled Laptops," IEEE International Symposium on Antennas and Propagation, Honolulu, Hawaii, USA, June 2007.

Introducing the Feature Article Authors

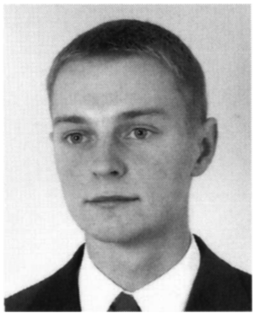

Jerzy Guterman is a Research Engineer in the Instituto de Telecomunicações (IT), Lisbon. He received the BS and MS degrees from Warsaw University of Technology, Poland (2002 and 2004), and the PhD summa cum laude from the Instituto Superior Técnico (2008). His research interests include small and multi-band antennas, antennas for laptops, electromagnetic human interactions, and MIMO antennas. From 2006 to 2007, he was a Visiting Researcher at the Antenna Research, Analysis, and Measurement Laboratory (ARAM), University of California, Los Angeles (UCLA), under the supervision of Prof. Yahya Rahmat-Samii. Before joining IT in 2004, he was a Research Assistant in the Institute of Radioelectronics, Warsaw University of Technology.

Dr. Guterman has authored and co-authored one book chapter and over 30 technical journal articles and conference papers. He received scholarships from the Foundation for the Development of Radiocommunication and Multimedia Technologies in Poland (2002-2004) and the Portuguese Research Council, FCT (2004-2008). He was awarded the 1st EuMA Microwave Prize at the 15th IEEE International Conference on Microwaves MIKON 2004, Poland, and the Best Student Paper Prize at the 6th Conference on Telecommunications, ConfTele 2007, Portugal. He is listed in *Who's Who in America.*

António A. Moreira received his PhD degree in Electrical Engineering from IST, Instituto Superior Técnico, Universidade Técnica de Lisboa, Portugal, in 1984. In 1989, he became an Associate Professor in the Electrical Engineering and Computer Department of IST. Since then, he has been responsible for antennas and radar systems courses. He also runs telecommunications and radar courses in the Portuguese Navy School. He is a researcher at the "Institute of Telecommunications," Lisbon, with his work being focused in antennas for wireless communications. He has participated in recent European Commission-funded projects, such as FLOWS (Flexible Convergence of Wireless Standards and Services) and ACE (Antenna Center of Excellence).

In recent years, Dr. Moreira has co-authored several journal and conferences papers in his current research topic of antennas for laptops, including antenna-integration issues, MIMO-enabled laptops, and electromagnetic-human interaction.

Custódio Peixeiro was born in Évora, Portugal, in 1956. He received the graduation, masters, and doctoral degrees in Electrical and Computer Engineering from the Instituto Superior Técnico (IST), Technical University of Lisbon, in 1980, 1985, and 1993, respectively. He has been teaching in the Department of Electrical and Computer Engineering since 1980, where he is now an Assistant Professor. He is also a researcher of the Instituto de Telecomunicações.

His present research interests are focused in microstrip antennas, and circuits for applications in mobile terminals (handsets, PDAs, and laptop computers).

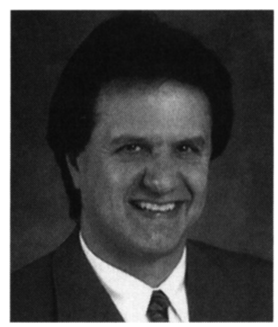

Yahya Rahmat-Samii received the MS and PhD degrees in Electrical Engineering from the University of Illinois, Urbana-Champaign. He is a Distinguished Professor and past Chair of the Electrical Engineering Department, University of California, Los Angeles (UCLA). He was a Senior Research Scientist with the National Aeronautics and Space Administration (NASA) Jet Propulsion Laboratory (JPL), California Institute of Technology, prior to joining UCLA in 1989. In the summer of 1986, he was a Guest Professor with the Technical University of Denmark. He has also been a consultant to numerous aerospace companies. He has been Editor and Guest Editor of numerous technical journals and books. He has authored and coauthored more than 660 technical journal and conference papers, and has written 20 book chapters. He is a coauthor of *Implanted Antennas in Medical Wireless Communications* (Morgan & Claypool, 2006), *Electromagnetic Optimization by Genetic Algorithms* (Wiley, 1999), and *Impedance Boundary Conditions in Electromagnetics* (Taylor & Francis, 1995). He has received several patents. He has made pioneering research contributions in diverse areas of electromagnetics, antennas, measurement and diagnostics techniques, numerical and asymptotic methods, satellite and personal communications, human/antenna interactions, frequency-selective surfaces, electromagnetic-bandgap structures, applications of genetic algorithms, and particle-swarm optimization.

Dr. Rahmat-Samii is a member of the US National Academy of Engineering, a Fellow of the IEEE, a Fellow of the Institute of Advances in Engineering (IAE), a member of Commissions A, B, J, and K of USNC/URSI, and a member of the Antenna Measurement Techniques Association (AMTA), Sigma Xi, Eta Kappa Nu, and the Electromagnetics Academy. He was Vice President and President of the IEEE Antennas and Propagation Society in 1994 and 1995, respectively. He was an IEEE AP-S Distinguished Lecturer. He was a member of the IEEE Strategic Planning and Review Committee (SPARC). He was the IEEE AP-S Los Angeles Chapter Chair (1987-1989): his Chapter won the Best Chapter Awards in two consecutive years. He is listed in *Who's Who in America*, *Who's Who in Frontiers of Science and Technology*, and *Who's Who in Engineering*. He designed the IEEE Antennas and Propagation Society (IEEE AP-S) logo. He was a Director and Vice President of AMTA for three years. He has been Chair and Co-Chair of several national and international symposia. He was a member of the University of California at Los Angeles (UCLA) Graduate Council for three years. He has received numerous NASA and JPL Certificates of Recognition. In 1984, he received the Henry Booker Award from URSI. Since 1987, he has been designated every three years as one of the Academy of Science's Research Council Representatives to the URSI General Assemblies held in various parts of the world. In 1992 and 1995, he received the Best Application Paper Prize Award (Wheeler Award) for papers published in the 1991 and 1993 *IEEE Transactions on Antennas and Propagation*. In 1999, he received the University of Illinois ECE Distinguished Alumni Award. In 2000, he received the IEEE Third Millennium Medal and the AMTA Distinguished Achievement Award. In 2001, he received an Honorary Doctorate in Physics from the University of Santiago de Compostela, Spain. In 2001, he became a Foreign Member of the Royal Flemish Academy of Belgium for Science and the Arts. In 2002, he received the Technical Excellence Award from JPL. He received the 2005 URSI Booker Gold Medal, presented at the URSI General Assembly.

To All IEEE Life Members

Life Member status in the IEEE is an earned honor. Each year, most Life Members are sent a Life Member Profile in lieu of a membership dues invoice. **Life Members must return the Profile**, indicating that they wish to keep their membership(s) active, even if there are no changes. **If the profile is not returned, it is assumed that their membership should not be kept active, and they do not receive any complimentary Society publications to which they may be entitled.** If applicable, the complimentary Society publications that a Life Member would like to continue receiving must be indicated on the Profile. Life Members can still retain their membership in a Society, even if they do not wish to receive its publications. However, they *must* return the Profile.

The Profile can also be updated online at www.ieee.org/renewal, or by logging into "myIEEE" at http://www.ieee.org/web/membership/home/index.html, using an IEEE Web account. Those not having an IEEE Web account can register for one at www.ieee.org/web/accounts/.

Getting the *Magazine* by Air Freight

Air freight delivery of the *IEEE Antennas and Propagation Magazine* is available to subscribers in IEEE Regions 8-10. The cost was recently $44.00 per year. This can be added to a member's subscription (and the current cost verified) via the Web at http://www.ieee.org/web/aboutus/help/member_support.html.